Review on fiber-optic sensing in health monitoring of power grids

Quan Chai
Yang Luo
Jing Ren
Jianzhong Zhang
Jun Yang
Libo Yuan
Gang-Ding Peng

Review on fiber-optic sensing in health monitoring of power grids

Quan Chai,[a] **Yang Luo,**[a] **Jing Ren,**[a] **Jianzhong Zhang,**[a,*] **Jun Yang,**[a,*] **Libo Yuan,**[a] **and Gang-Ding Peng**[b]
[a]Harbin Engineering University, School of Science, Key Laboratory of In-Fiber Integrated Optics of Ministry of Education, Harbin, China
[b]University of New South Wales, School of Electrical Engineering and Telecommunications, Photonics and Optical Communications, Sydney, Australia

Abstract. Fiber-optic sensing technology is best adapted to health monitoring and evaluation of power grids because of its immunity of electromagnetic interference, capabilities of multiplexing and distributed sensing, and tolerance to harsh environments. We review key fiber-optic sensing technologies, including fiber Bragg gratings, fiber-optic interferometers, optical time domain reflectometries, and their applications in three main parts of power grids, transformers, power towers, and overhead transmission lines, during the past 20 years. In particular, optical fiber composite overhead ground wire and optical phase conductor applied in power grids are the areas of great potential to go further. The perspectives of an intelligent fault diagnosis subsystem for power grids based on a fiber-optic sensing network are discussed, and related on-going work is described. The review shall be of benefit to both engineers and researchers in power grids and fiber-optic sensing. © *2019 Society of Photo-Optical Instrumentation Engineers (SPIE)* [DOI: 10.1117/1.OE.58.7.072007]

1 Introduction

Power generating stations are usually located near energy sources, such as coal mines, dam sites, or renewable energy farms. Power grids are interconnected networks for delivering electricity from stations to consumers.[1] A power grid usually consists of transformers, power towers, overhead transmission lines and distribution lines, many other components including circuit breakers, disconnectors, surge arrestors, etc. The electric power which is generated is stepped up to a high voltage at which it connects to the overhead transmission lines. On arrival at a substation, the power will be stepped down from a transmission level voltage to a distribution level voltage by transformers. The power tower is a tall structure, usually a steel lattice tower, used to support an overhead transmission line. Finally, the power is stepped down again from the distribution voltage to the required service voltage.[1] The losses caused by natural disasters (e.g., rainstorm, snowstorm, and thunder striking) to the power grid are enormous. It is thus of great significance to form an intelligent fault diagnosis system for the health monitoring and evaluation of a power grid in real time.

The different parts of a power grid have their respective major failure causes. For transformers, electrical and thermal stresses always occurred and induced their breakdown. The gas voids (voids in solid epoxy insulation or bubbles in transformer oil) caused by the electrical and thermal stresses will induce partial discharge. Protracted partial discharge is a sign used to evaluate the fault possibility. The waste heat generated in transformer operation causes temperature rise in the internal structures of the transformer, which would generate hydrogen (H_2). The abnormity of temperature and H_2 concentration are two early signs for the potential failure of transformers as well. Power towers are threatened by landslides, debris flows, erections of foundation settlement, lines galloping, and so on, which induce considerable strain, tilt, and deformation of the power towers. Overhead transmission lines are easily suffered from the impact of complex meteorological and geographical conditions, which may cause short circuits and open circuits. Galloping, windy, icing, temperature of transmission lines are the main objects of observation.

Fiber-optic sensing technology has developed rapidly in the past 30 years. It has been widely used in the monitoring of structural health,[2–4] geology,[5–7] industrial engineering,[8,9] aircraft,[10,11] environment,[12,13] and so on.[14,15] Due to its advantages, including immunity of electromagnetic interference, capabilities of multiplexing and distributed sensing, and tolerance to harsh environments, fiber-optic sensing technology is a suitable option for the applications in power grids. On the other hand, optical fiber composite overhead ground wire (OPGW) and optical phase conductor (OPPC) are used extensively as power transmission lines, which prove the priority of the fiber-optic sensing technology naturally.[16]

For the past 20 years, there have been many reports about the applications of fiber-optic sensing in power grids. However, there are few papers to give a comprehensive review of this important application area even though many excellent review papers of fiber-optic sensors have been given.[17–22] This paper is given to fill the gap. It would be benefit to the researchers in power grid to know fiber-optic sensing technologies used already and also gives a shortcut for the researchers in fiber-optic sensing to know the requirements and huge potential market in power grid.

This review paper is arranged as follows: fiber-optic sensing technologies used in power grids are introduced briefly in

*Address all correspondence to Jianzhong Zhang, E-mail: zhangjianzhong@hrbeu.edu.cn; Jun Yang, E-mail: yangjun@hrbeu.edu.cn

the first part of Sec. 2. Then we review fiber-optic sensing applications in the main components of a power grid, including transformers, power tower, and overhead transmission lines, which is the second part of Sec. 2. In Sec. 3, the perspective and consideration types of optical fiber sensors working collaboratively to form an intelligent early fault diagnosis subsystem are discussed and one on-going project as an example of cases is described. This paper ends up with a brief conclusion.

2 Fiber-Optic Sensing Applications in Power Grid

This section will review the fiber-optic sensing technologies, including fiber Bragg grating (FBG), fiber-optic interferometer, distributed fiber-optic sensing, and power grid. Transformers, power tower, and overhead transmission lines are three key components of a power grid as shown in Fig. 1. Two main failure causes of a transformer are electrical and thermal stresses, which can be monitored by partial discharge and the abnormity of temperature and gases, H_2 typically. The geology/weather-induced strain, tilt, and deformation of power towers can be measured by fiber-optic sensors. The short circuit or open circuit of transmission lines may be evaluated by the measurements of temperature, icing, and galloping. Fiber-optic-interferometer-based sensors can be designed with super high sensitivity, but they are used to detect partial discharge. FBGs have been widely used in all types of applications because of their ultrastrong multiplexing capability and appeared to be one of the best commercialized optical fiber devices. Distributed fiber-optic sensors have been practiced in most applications as well and prove to be one of the most promising sensing schemes because of OPPC/OPGW used extensively in power grids.

2.1 Brief Introduction of Fiber-Optic Sensing Technology

First, we introduce briefly the principles of fiber-optic sensing technologies used widely in power grid monitoring. The principles of these types of fiber-optic sensors can be summarized in two categories: point sensor and distributed sensor. A point fiber-optic sensor produces measurement data at certain locations according to where its specific sensing components are, whereas the distributed fiber-optic sensor produces the measurement data of the spatial and temporal domains across long distances. The point sensor has a variety of configurations such as FBG and some types of fiber-optic interferometer. The distributed fiber-optic sensing technology including optical time-domain reflectometry (OTDR), phase sensitive optical time-domain reflectometry (Φ-OTDR), Brillouin optical time-domain reflectometry (B-OTDR), the stimulated Brillouin optical time-domain analysis (B-OTDA), and Raman optical time-domain reflectometry (R-OTDR).

2.1.1 Fiber Bragg grating

FBG is a periodic and permanent modification of the core refractive index value (typically 10^{-5} to 10^{-3}) along the optical fiber axis.[23–25] Two counter-propagating core modes will be coupled, which cause a Bragg reflection (shown in Fig. 2) and the Bragg wavelength can be expressed as

$$\lambda_B = 2n_{\text{eff}}\Lambda, \qquad (1)$$

where n_{eff} is the effective refractive index of the core mode at the Bragg wavelength, and Λ is the period of the FBG. FBG can be used as a temperature or strain sensor by observing the Bragg wavelength changed by strain or temperature.
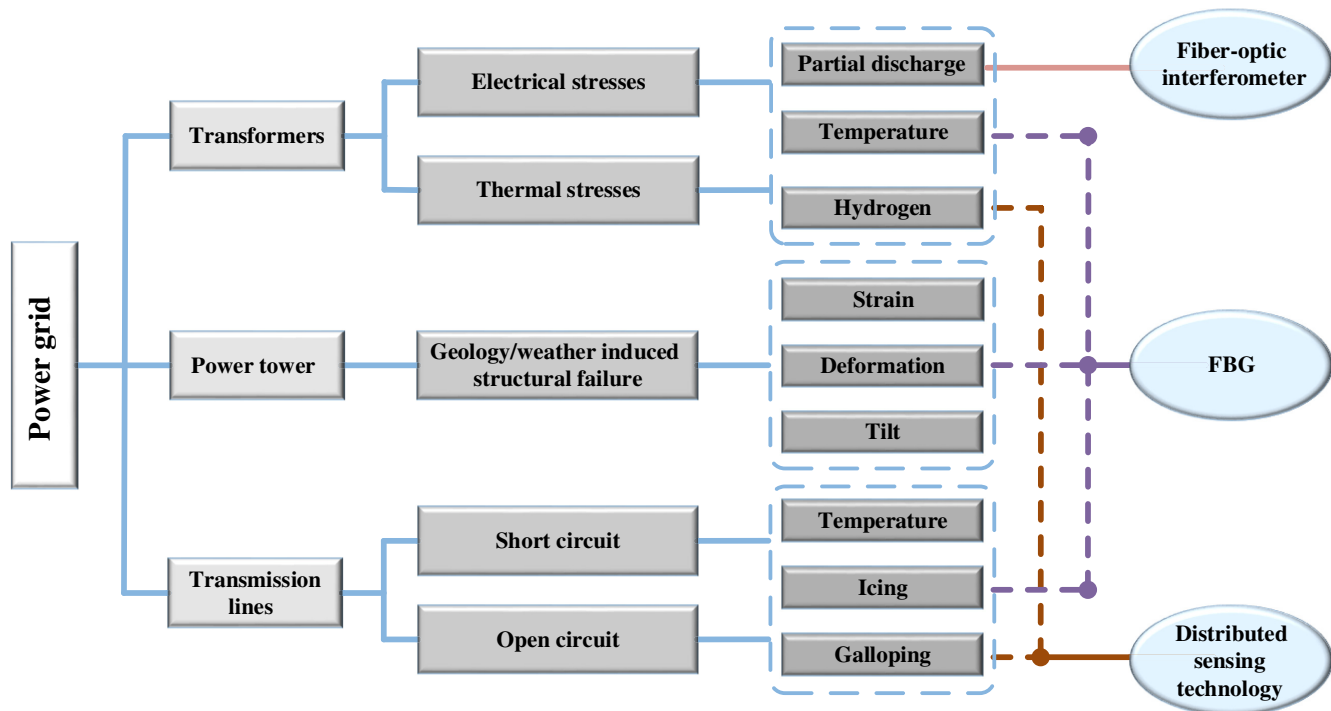

Fig. 1 The structure of the power grid and the fiber-optic sensing technology mostly applied in power grid.
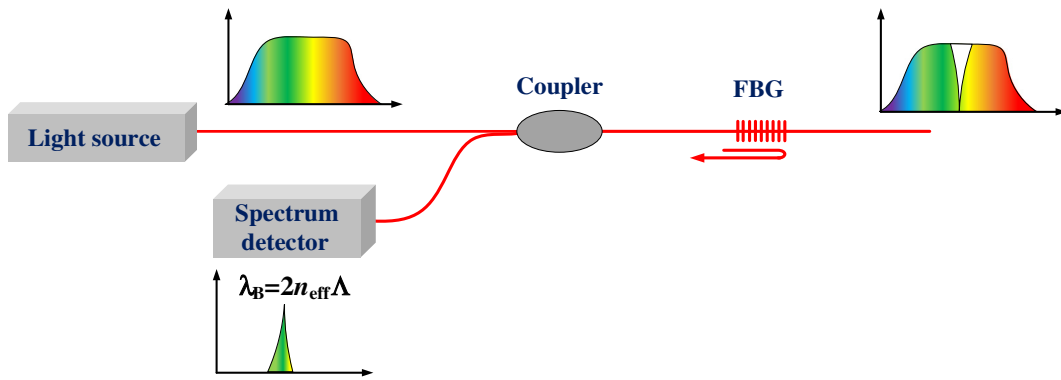
Fig. 2 Schematic of an FBG.

For an FBG inscribed in standard SMF-28, the strain and temperature sensitivity is about 1.2 pm/$\mu\varepsilon$ and 13.5 pm/°C around 1550 nm, respectively.[24]

The main advantage of FBG is an absolute measurement and independent of the light fluctuating. Due to the narrowband reflective spectrum and the low insertion loss, FBG arrays are easily constructed along a single-mode fiber (SMF). The excellent multiplexing capability is beneficial for distributed sensing or quasidistributed sensing. Nowadays, FBGs play more and more important roles in sensing applications.

2.1.2 Fiber-optic interferometer

Fiber-optic interferometer is a common technology in sensing areas. In most fiber-optic interferometers, light is split into two beams that propagate in different optical paths then combined again.[26] The output light contains information about the optical path difference and is displayed as a cosine function. The phase difference $\Delta\Phi$ can be described as

$$\Delta\Phi = \frac{2\pi}{\lambda}\Delta(nL),\tag{2}$$

where $\Delta(nL)$ is the optical path difference, and λ is the wavelength. For sensing applications, one of the beams is isolated from the environment variations to work as a reference arm, and the other is used to detect the variations of the environment, which is named as a sensing arm. The optical path difference changed by the environmental variations will move the interference fringe, which is used as sensing scheme.

Based on different working principles, a fiber-optic interferometer can be categorized into a Mach–Zehnder interferometer (MZI), Michelson interferometer (MI), Fabry–Perot interferometer (FPI), and Sagnac interferometer (SI).

As shown in Fig. 3(a), an MZI works in a transmission mode. The light is launched into the fiber and then coupled into two fibers by a coupler. The other coupler is used to combine the light in two fibers to realize the interference. The in-line MZI-based sensors have been rapidly developed due to their compact configurations and designable functions. They usually operate with two modes and realized interference in one fiber, eliminating the need for couplers. Nowadays, some typical configurations have been designed using long-period grating (LPG), SMF, photonic crystal fiber (PCF), and tapered fibers.[27–31]

The MI works in a reflection mode as shown in Fig. 3(b). The MI sensor generally required a mirror element to reflect the light at the end of fiber. Some typical in-line MI configurations are also designed using LPG, PCF, twin-core fiber, and so on.[32–35]
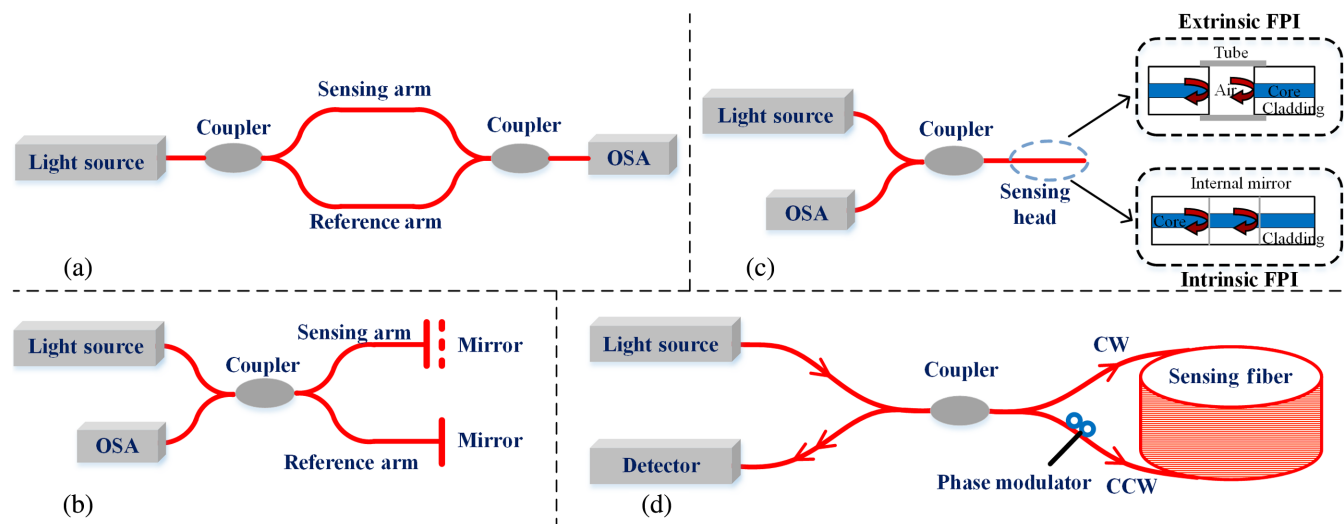

Fig. 3 Schematic of fiber interferometers: (a) MZI, (b) MI, (c) FPI, and (d) SI.

An FPI is generally composed of two parallel reflecting surfaces separated by a certain distance (called an etalon).[36] Two reflected beams form an interference fringe. Two categories of FPI sensors, extrinsic FPI (EFPI) and intrinsic FPI (IFPI), are shown in Fig. 3(c) according to the reflectors outside or inside the fiber. The EFPI could obtain a high-finesse interference signal by utilizing high reflective mirrors.[37] The inside reflector of IFPI sensor could be formed by micromachining, FBG, chemical etching, and thin film deposition.[38–41] It is important to design an etalon length of FPI-based sensor to balance the requirements of sensing range and sensitivity in applications.

Different from the above fiber interferometers, an SI is formed by an optical fiber loop. As illustrated in Fig. 3(d), the input light is divided into two directions by a coupler and the clockwise and counter-clockwise propagating light combined again by the same coupler.[42] The output spectrum contains the beating frequency of the two counter-propagating light if the fiber coil is rotated. Nowadays, SIs has been applied in various sensing applications and fiber-optic gyroscopes[43] may be the most significant.

2.1.3 Distributed fiber-optic sensing technology

For distributed fiber-optic sensing technology, the fiber optical itself acts as a continuous array of sensors. The environmental perturbation affects the parameters of the core of fiber, such as optical length, diameter, and refractive index, which modulate the backscattered light, including its intensity, phase, and frequency. Monitor the backscattered light of the fiber, the surrounding environment perturbations can be figure out.

The backscattering can be categorized as Rayleigh, Brillouin, and Raman, which are shown in Fig. 4. Rayleigh scattering is caused by the inhomogeneity of the fiber core and the backscattered Rayleigh light has the same the wavelength with the input light.[44–47] Brillouin scattering is caused by an acoustic wave from lattice vibration, which is the interaction between the input light and the phonon.[47] The Brillouin backscattering is usually about 15 and 20 dB weaker than the Rayleigh backscattering and has a frequency shift ~11 GHz for SMF around 1550 nm. This frequency shift is sensitive to temperature and strain.[48] Spontaneous Raman scattering is caused by the phonons[49] and about 10 dB weaker than the spontaneous Brillouin scattering.
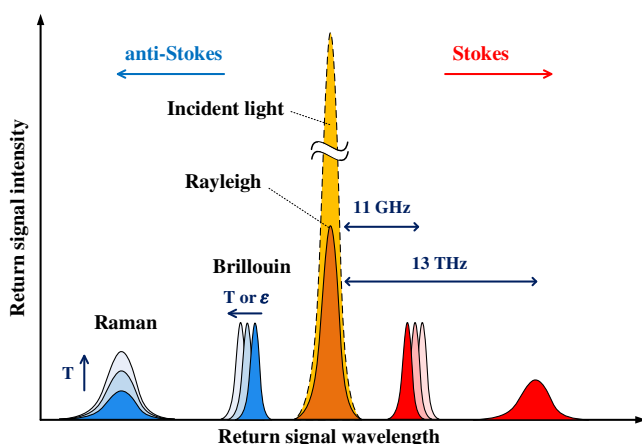

Fig. 4 Typical spontaneous scattering spectrum in an optical fiber.

A frequency shift ~13.0 THz with a wide bandwidth of ~6 THz is much larger than that of the Brillouin scattering. The intensity of Stokes signal is temperature insensitive, whereas the anti-Stokes signal is temperature sensitive. Therefore, the Raman scattering light can be used to temperature measurement.[50] Some distributed sensing technologies based on the scattering mechanisms are introduced here briefly.

OTDR. Since demonstrated by Barnoski and Jensen,[51] OTDR has become a commercial instrument to characterize an optical fiber. The working principle of OTDR is illustrated in Fig. 5. A short optical pulse is launched into the fiber and monitoring the attenuation of the backscattered signal by a detector.[52,53] The Rayleigh backscattering light should be decayed exponentially with time. The external perturbations (e.g., bending, break-induced end face, or introduce a connector) applied on the fiber will be changed the attenuation at the perturbation location. The attenuation of Rayleigh backscattered light is used for distributed sensing along the fiber.

The spatial resolution of an OTDR is defined as $c\tau/2n$. c and n are the light velocity in vacuum and refractive index of optical fiber, respectively. τ is the bandwidth of the input pulse. The lower the bandwidth of the input pulse, the higher the spatial resolution. However, it means lower pulse power, which decrease the signal-to-noise ratio (SNR) of OTDR and is a serious problem for long-range sensing. Therefore, it is important to optimize the bandwidth of pulse to satisfy the spatial resolution and the sensing range in application. In addition, the response time of the detector is usually several nanoseconds, which also limited the spatial resolution of OTDR.

Φ-*OTDR.* The Φ-OTDR technique was first proposed by Taylor and Lee[54] by detecting the intensity changes of the interferometric light and has become an effective tool for distributed vibration and intrusion sensing nowadays.[55–58] Different from OTDR, Φ-OTDR requires a highly coherent laser with narrow line width. The output signal of Φ-OTDR is modulated by the coherent interaction of numerous scattering centers within the pulse duration. The working principle of the Φ-OTDR is shown in Fig. 6. When a perturbation is applied on a sensing fiber, the phase will change at the position due to the change in refractive index and length of the fiber. This induces the intensity change corresponding to the time or the position. The backscattered Rayleigh light is launched into an interferometer system, such as an imbalanced MI (or MZI). The output interference signal is split into three signals differing by $2\pi/3$ phase delay by a 3×3 coupler. Three PDs detect the signals and a data acquisition card saved the signals. Then the perturbation can be identified by proper demodulation algorithm. Similar to OTDR, the spatial resolution and the sensing range need to be balanced. Another challenge for Φ-OTDR is the polarization mismatch, which could reduce the probability of detecting perturbation points and result in wrong signals.

B-OTDR and B-OTDA. The Brillouin scattering-based distributed sensing was focused on temperature and strain measurement.[59–62] Brillouin scattering-based sensors are categorized as the B-OTDR and B-OTDA.
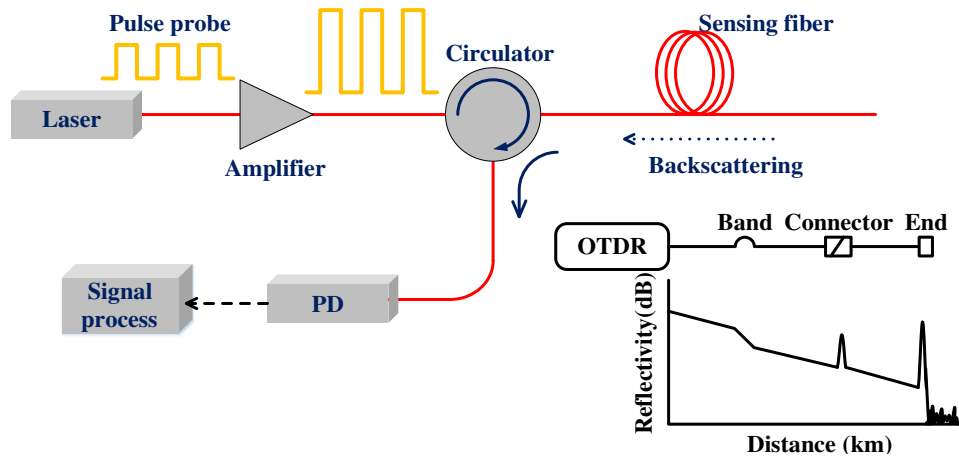
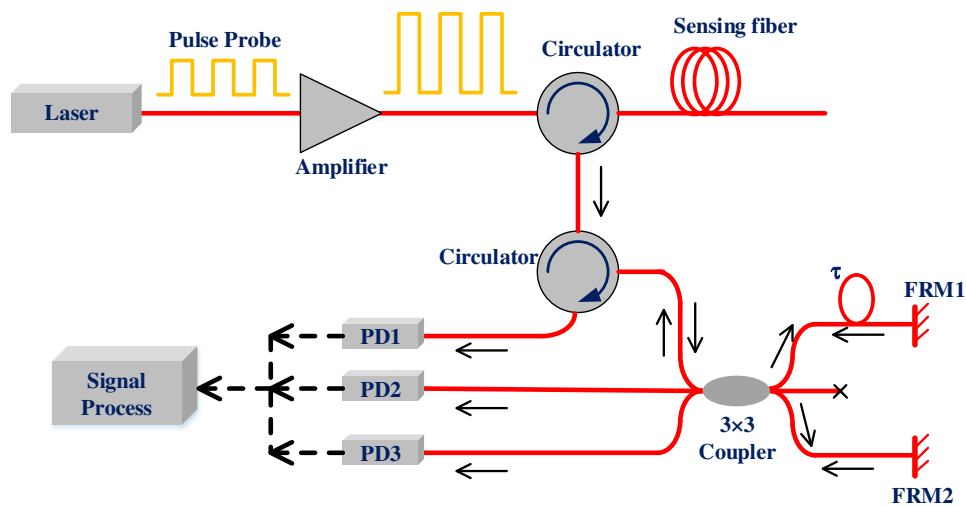**Fig. 5** The principle of operation of the OTDR.

Fig. 6 The principle of operation of the Φ-OTDR.

B-OTDR is based on spontaneous Brillouin scattering and was initially introduced to enhance the working range of OTDR.[63] The operation principle of B-OTDR is shown in Fig. 7. A pulsed laser launched optical pulse into the sensing fiber and generate spontaneous Brillouin scattering. A local laser generates continuous wave (CW) light to act as the heterodyne light. The heterodyne light is mixed with the scattered light. The detector is receiving the coherent signal. Despite that the back scattered signal is weak, it can be work even if the fiber is broken, which is suited for industrial applications.[64] B-OTDA is based on stimulated Brillouin scattering. As shown in Fig. 8, a pulse laser and a CW laser launched light to both ends of the fiber. To detect the weak counter propagating Brillouin scattering signal, a coherent detection technique is adopted.[65] When the frequency difference of the CW signal and the input pulse is equal to the Brillouin frequency shift, stimulation of the Brillouin scattering occurs.[53,66] B-OTDA measures the gain of the two counter propagating waves and improves the performance. However, it does not work when the loop is broken at any point of the fiber.

R-OTDR. Since being proposed in the 1980s,[50,67] Raman-based sensing systems have widely been used in distributed temperature measurement. The operation principle of R-OTDR is illustrated in Fig. 9. A pulsed laser source launched a pulse into the fiber. The detector used to measure the back-scattered Stokes and anti-Stokes band responses over a roundtrip propagation. A section of fiber that knows the temperature is inserted between the coupler and sensing fiber for temperature calibration. In principle, there are some limitations with the types of fiber in R-OTDR systems. For multimode fiber, the intermodal dispersion will broaden the pulse signal and reduce the spatial resolution. For SMF, a high-performance laser source and anti-Stokes photodetector are required because the wavelength of anti-Stokes signal should be larger than the cut-off wavelength of the fiber (~1310 nm for standard SMF). For example, an R-OTDR sensing system based on 15-km SMFs requires the detector working long wavelengths, such as InGaAs photodetectors.[68]

2.2 Fiber-Optic Sensing Applications in Transformers

Transformers play an important role in power system networks. They regulate voltage levels for safe, reliable, and economic transmission and distribution of electrical energy from power generating stations to utility end. A schematic diagram of the fiber sensor in the transformer is shown in
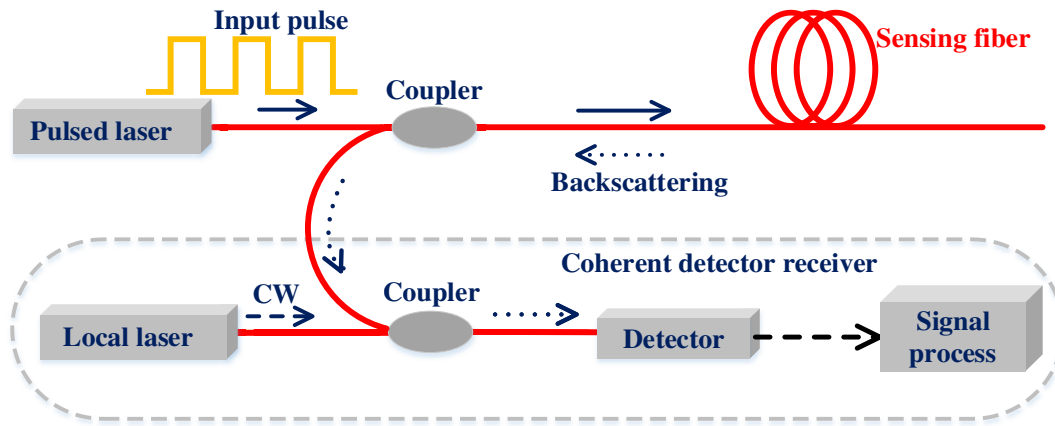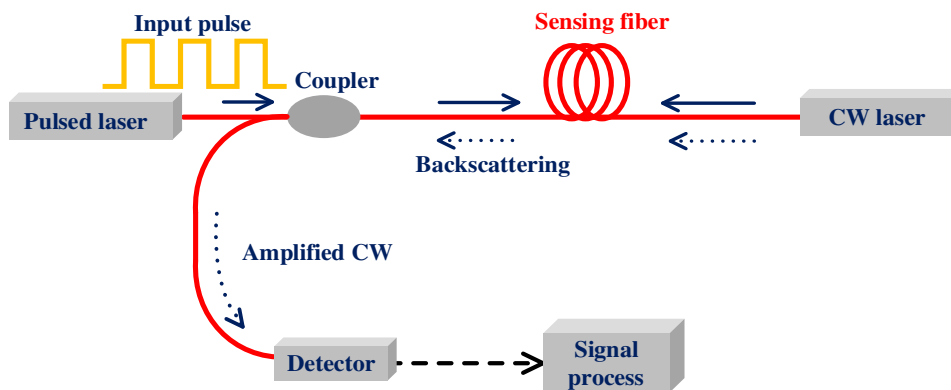
Fig. 7 The principle of operation of the B-OTDR.

Fig. 8 The principle of operation of the BOTDA.
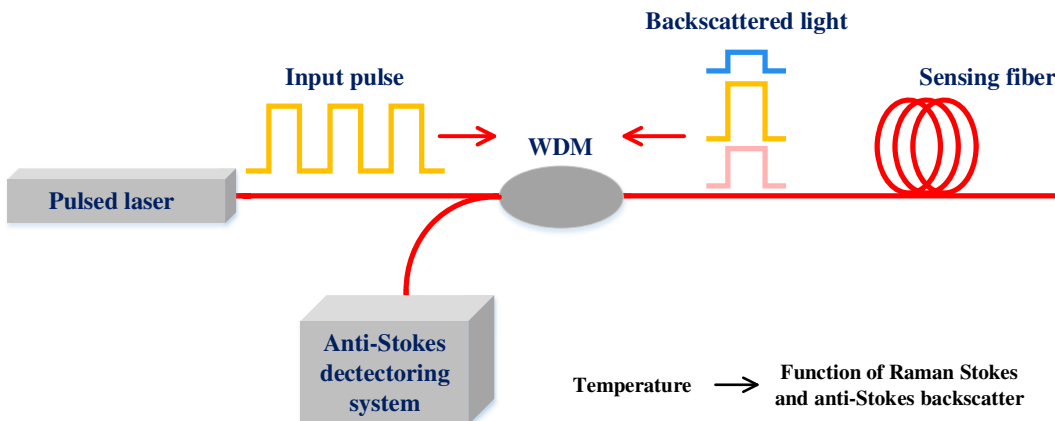
Fig. 9 The principle of operation of the R-OTDR.

Fig. 10. Large power transformers have a normal life expectancy of 60 years if routine maintenance is performed.[21] Despite this, electrical and thermal stresses always occurred during long service period, which could induce in-service failures. It is essential to monitor the condition of a transformer to avoid premature malfunction or breakdown. Monitoring partial discharge, temperature of oil and winding, and H_2 concentration are the solutions for an early detection of potential failures.

2.2.1 *Partial discharge monitoring*

Partial discharge is defined as a localized dielectric breakdown under high-voltage stress, which bridges the insulation between two conductors.[69] It is the main phenomenon that causes the degradation of insulation of high-voltage power transformers. To ensure the safety of power transmission, partial discharge measurements are an effective method of monitoring the condition of power transformers.

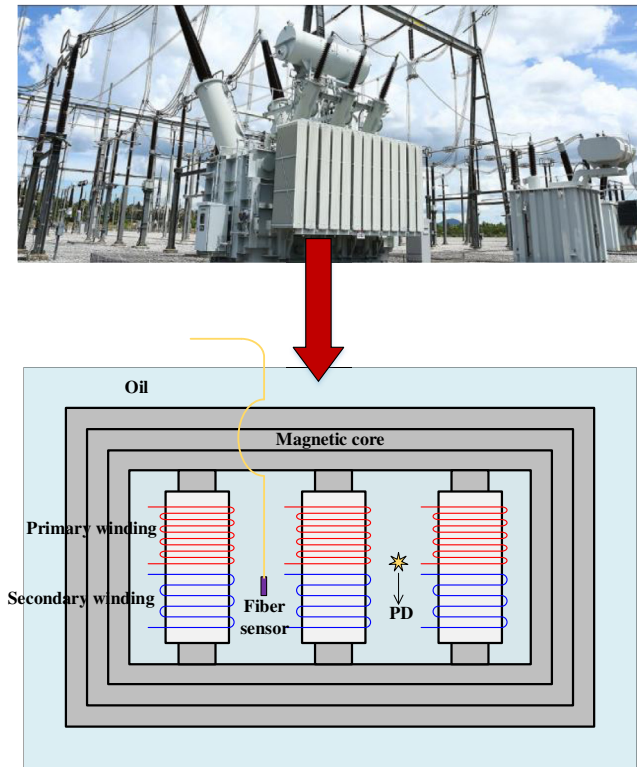**Fig. 10** Schematic diagram of fiber sensor in transformer.

Partial discharge generates mechanical stress waves that propagate through the surrounding oil in the range of 100 to 300 kHz.[21] To detect these waves, acoustic emission detection methods are the most used in partial discharge monitoring. Compared with ultrahigh frequency method, the acoustic detection method is immune to electromagnetic interference, and it is easy to locate the insulation defect with the detected signal. Optical fiber as a dielectric material can be easily placed directly into the power transformer to get close to the potential partial discharge source, enabling it to diagnose small defects. Many investigations demonstrated the excellent characteristics of optical fiber sensor in partial discharge monitoring.

Interferometric sensors have been widely investigated in partial discharge monitoring. Some researchers used MZI to detect partial discharge by acquiring acoustic signals.[70–73] Based on all fiber MZI and homodyne demodulation, 1.3-Pa acoustic pressure can be detected in a transformer.[72] A multi-channel heterodyne interferometer capable of processing four channels simultaneously is applied to locate the partial discharge position.[73] An MI-based sensor with a high SNR and flat response between 20 to 150 kHz is used to monitor the partial discharge.[74] EFPI sensors[75–78] have been used by some researchers to detect partial discharge due to its compact size and realize single-point measurement. It is need to note that at the same conditions, the EFPI configuration had a better performance compared with the IFPI sensor.[79] Due to truly path-matched interference mode, Sagnac interferometric sensor shows its stability against environmental temperature influences and attracted researchers' interest. Based on the fiber-optic SI, internal acoustic pressure and vibration due to the partial discharge in the transformer was monitored.[80] A fiber-optic acoustic sensor

was reported using a balanced Sagnac sensor and an EDFA-based fiber ring laser with the degree of polarization tunable function. The experimental results showed its feasibility to monitor high-frequency acoustic pressure to 300 kHz.[81]

FBG sensor[82–84] is also used widely because of its multi-plexing capability and small size. Due to impulsive acoustic pressure generated during partial discharge, detecting the wavelength shift of FBGs is a solution for partial discharge monitoring.[82] The intensity demodulation method based on FBGs and a wide band laser is also suitable for partial discharge monitoring.[83] This type of partial discharge detection system does not require either an FBG analyzer or a narrow band tunable laser source. However, the sensitivity of the system was not very high. FBGs combined with FPI configuration can improve the sensitivity of detecting the weak pressure.[84] Another method to improve the sensitivity is to use a phase shift FBG (PS-FBG).[85,86] Because the PS-FBG exhibits a sharp resonance, the ultrasonic sensitivity is improved compared with the FBG. It has been reported that the sensitivity of PS-FBG-based ultrasonic sensor is 8.46 dB higher than PZT sensor between 50 to 400 kHz.[86]

2.2.2 Temperature monitoring

The undesirable heat radiation in the transformer weakens the insulation of transformers, which causes faults in the high probability. The transformer losses are among the most important factors in rising of top oil and hot-spot temperature (HST). This causes rapid thermal degradation of insulation. HST, the highest temperature on the oil or winding, is the most important parameter of the transformer's life calculation. Industry standards limit maximum allowable HSTs in transformers to 140°C with conventional oil insulation.[21]

Traditional calculation and measurement of temperature distribution inside power transformers including calculation formula for HST,[87] finite-element method,[88] analytical methods,[89,90] and diagnostic measurements.[91] Optical fiber sensors are a better choice for temperature monitoring in power transformer for the reasons of electromagnetic interference and intrinsic safety. The Raman scattering-based sensing technology can realize a distributed temperature sensing (DTS) along the whole optical fiber. The temperature distribution along the winding of a 22-MVA in an oil-cooled power transformer was measured by DTS technology,[92,93] shown in Fig. 11. It is a trend for the temperature measurement in transformer.
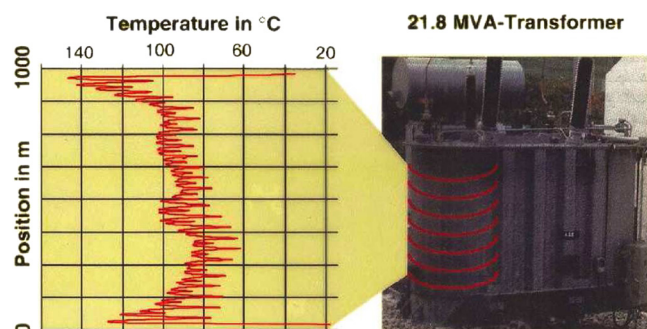

Fig. 11 Fiber-optic distributed temperature measurements along the windings in a power transformer.[93]

The FBG array is another choice to realize quasi-DTS in power transformer, which overcome the long acquisition time and the lower sensitivity of DTS system. An FBG temperature sensor achieved temperature measurement within the transformer winding.[94,95] Hot-spot measurements based on FBG sensors were realized on the power transformers of 25 kVA,[96] 154 kV,[97,98] 31.5 MVA/110 kV,[99] and 35 kV/4000 kVA.[100] Optical fiber sensors have much lower error deviation compared with that of Pt100 resistance thermometers.[101]

2.2.3 Hydrogen monitoring

In a transformer, oil worked as insulation, coolant, as well as the condition indicator will generate gasses, such as H_2, ethane (C_2H_6), methane (CH_4), acetylene (C_2H_2), ethylene (C_2H_4), carbon monoxide (CO), and carbon dioxide (CO_2) when the electrical or thermal stresses are accumulated to a certain degree. The fault gases in the transformer oil will reduce its insulation. The gases abnormity is the first evidence of an incipient fault in a transformer. For example, the abnormal C_2H_6 and C_2H_4 concentrations often mean there is thermal fault <300°C and between 300°C to 700°C, respectively, while the abnormal H_2 concentration means a partial discharge or a thermal fault between 150°C to 300°C.[21] According to the IEEE standards,[102] the concentrations for these key gases and the corresponding status of the transformers are listed in Table 1.

The traditional methods to analyze the dissolved gases in transformers including the chromatography,[103,104] spectroscopy,[105,106] and gas sensors.[107–110] Some electrochemical sensors based on semiconducting metal oxides have been utilized to gas sensing.[107–110] Optical fiber gas sensors attract people's interest due to its low cost, simple structure, and immunity to electromagnetic interference. Nowadays, optical fiber sensors have realized monitoring these gases of concern, such as CH_4,[111–114] C_2H_2,[115,116] and H_2, in transformer oil. Among these gases, H_2 especially in Ref. 117, provides a clearer insight in the health condition of a transformer and allows for an early failure evaluation.

The H_2 concentration sensors need to meet the following specifications to provide a continuous monitoring of the condition of power transformer. They should work from environment temperature to at least 110°C. The H_2 concentration detection range should be from 100 to 1000 ppm. Selectivity toward H_2 is crucial to avoid false alarms.[118]

The main types of fiber-optic sensing schemes, FBG-,[119–125] modified FBG-,[126–129] reflection,[130,131] and interferometer-[132] based are all by coating Pb-film on fiber as shown in

Figs. 12(a)–12(d), respectively. For FBGs coating with the Pd-based film, the expansion of the Pd-based thin film induced by the H absorption would introduce the stress on FBGs and their Bragg wavelength may shift, which is used as the sensing scheme. The thickness of Pd films shows different responses.[119] An FBG hydrogen sensor based on Pd/Ag composite film displays better stability than that of the pure Pd film.[120,121] Optimizing the microstructure by reducing the grain size or thickness of the films can improve the sensor performance. Pd/Au film[122] and Pd/Cr film[123]-based FBGs hydrogen sensors were also reported. A polymer coating is added as an intermediate layer to improve the poor adhesion between the thick Pd film and optical fiber.[124,125] To improve the sensitivity, a D-shaped FBG sensor-coated with a Pd thin film by magnetron sputtering was reported to test dissolved H_2 in transformer oil.[126] A high sensitivity of 1.96 ppm at every 1-pm wavelength shift was demonstrated in the range of 0 to 719.7 ppm of dissolved H_2.

Some literature reported a side-polished FBG-based hydrogen sensor, whose scheme is illustrated in Fig. 12(b). Due to its intrinsically sensitive to curvature, side-polished FBG can improve the sensitivity of H_2 sensing. Compared to a standard FBG coated with the same WO_3-Pd film, the side-polished FBG can increase the sensitivity of the sensor by >100%.[127] The sensitivity of a Pd/Ag composite film-based side-polished FBG sensor is about 11.4 times the conventional FBG sensors.[128] Like the structure of the side-polished FBG, the sensitivity of a 16-μm chemically etched FBG-based hydrogen sensor is improved by >30%.[129]

For reflection-based sensors,[130,131] as shown in Fig. 12(c), the Pd film is coated at the end face of an optical fiber and its reflectivity is changed due to the H_2 absorption. WO_3-Pd_2Pt-Pt composite film[130] coated on the end face of the optical fiber exhibited a detection limit of 20 ppm in air at 25°C. The filtering function of Pd_2Pt-Pt catalyst layer provided a good selectivity against 2% CH_4 and 1% CO. A polytetrafluorethylene-Pd (PTFE-Pd) thin film-based fiber-optic sensor[131] was demonstrated to measure the dissolved H_2 concentration. The results indicated that a larger range of H_2 concentrations could be measured at higher temperatures, which are more relevant for the temperature of an operating power transformer.

A PCF modal interferometer-based H_2 monitoring sensor for power transformer was also demonstrated.[132] As shown in Fig. 12(d), when the Pd/WO_3 film coated on the PCF surface absorbs H_2, the effective phase difference of interferometer was changed by the induced stress and the

Table 1 Dissolved gas concentrations for the key gases and total dissolved combustible gas (TDCG).

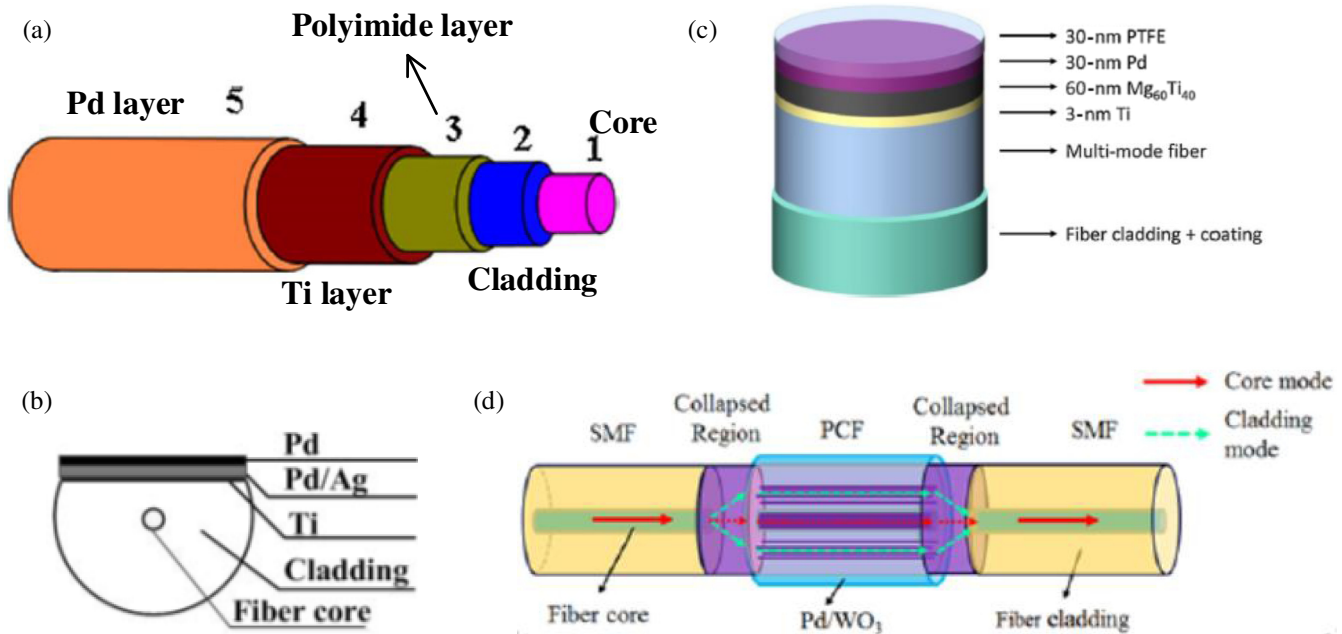| Status	Dissolved key gas concentration limits (ppm)							
	H_2	CH_4	C_2H_2	C_2H_4	C_2H_6	CO	CO_2	TDCG
Standard	100	120	1	50	65	350	2500	720
Caution	101 to 700	121 to 400	2 to 9	51 to 100	66 to 100	351 to 570	2500 to 4000	721 to 1920
Warning	701 to 1800	401 to 1000	10 to 35	101 to 200	101 to 150	571 to 1400	4000 to 10,000	1921 to 4630
Danger	>1800	>1000	>35	>200	>150	>1400	>10,000	>4630

Fig. 12 Schemes of fiber-optic H_2 sensors based on Pd-based films. (a) FBG,[114] (b) D-shape FBG,[128] (c) reflection-based sensor,[131] and (d) interferometer.[132]

resonant wavelength of interference spectrum was shifted. Experiment results showed a linear correlation between the resonant wavelength and the concentration of H_2 dissolved in the transformer oil and a sensitivity of about 0.109 pm/$(\mu L/L)$ with a response time of ~30 min.

In summary, partial discharge, temperature, and hydrogen abnormity induced by electrical and thermal stresses in transformers are the main early faults needed to be detected. As shown in Table 2, types of fiber-optic interferometers are suitable for partial discharge monitoring by detecting acoustic emission signals and FBG sensors with smaller size and stronger multiplexing capability are an alternative choice but with lower sensitivity. A distributed optical sensing system, mainly based on R-OTDR, is a solution in temperature monitoring with the accuracy of ~1°C, the spatial resolution of meter-level and the measurement time of second-level. Quasidistributed sensing technology, FBGs, with less measurement points is more suitable for the requirements of higher resolution of centimeter level, higher measurement speed of kilohertz level, and higher accuracy of ~1°C. Hydrogen in transformer oil has been monitored by Pb-film-coated optical fiber sensors. To improve their sensitivity and response, time optimizations are still focused on the film thickness, materials, and the structures of optical fiber sensors.

2.3 Fiber-Optic Sensing Applications in Power Tower

Power towers are used as the critical support units of conductors and ground wires. The unbalanced tension, even the tower collapse or the conductor disconnection shown in Fig. 13, may be caused by the loads of wind, icing, transmission line galloping, and so on. If the strain, tilt, and deformation of power towers can be monitored in real time, the towers can be strengthened and the occurrence of the tower collapse will be decreased greatly. The most widely used fiber-optic sensing technology in power tower is based on

FBG. Figure 13 shows a schematic diagram of power tower and FBG-based sensing system. FBG sensors are installed on the cross arms and tower body.

FBG strain sensors installed on the cross arm of the power tower of Yanjin transformer station[133] indicated that the transmission lines sweeping wind is the main reason to cause their deformation. Moreover, the earth pressure of power tower is seasonal change with the local precipitation.[134] FBG-based tower vibration was also demonstrated to satisfy the prealarm requirement.[135,136] Xie et al.[137–139] designed a 1000-kV double circuit tower-eight bundled conductors coupling system based on FBG sensors. The experiment results indicated that the dynamic tension should be considered in wind resistant design of tower-line coupling system. A power tower landslide monitoring system based on FBGs was applied in Maoxian.[140,141] The monitoring results indicated the power tower deformation was caused by a shallow and slowly moving landslide. The online monitoring technology of tower foundation deformation was developed based on the FBG stress sensor and successfully applied in Jibei Power Grid in China.[142] The results showed that the stresses fluctuating with the wind speed are small if the tower foundation is solid. Otherwise, the stresses were expected to vary drastically.

In summary, FBG-based sensing is a widely used technology in health monitoring of power towers, including their deformation, vibration, and the safety of tower foundation.

2.4 Fiber-Optic Sensing Applications in Overhead Transmission Lines

Overhead transmission lines are an important part of a power grid, which easily suffer from the impact of complex meteorological and geographical conditions. Many online monitoring schemes were developed to improve the reliability of transmission lines, such as temperature, icing, and galloping monitoring. To monitor those events, fiber-optic

Table 2 Optical fiber sensing applied in the power transformers.

Monitoring targets	Fiber-optic sensing technology		Advantages	Disadvantages
Partial discharge-induced acoustic pressure (100 to 300 kHz)	Interferometers	MZ Interferometer[70–73] MI[74]	High sensitivity and large flat response range	Difficult to multiplex
		FP Interferometer[75–79]		
		SI[80,81]		
	FBGs	FBG[82–84]	Easy to multiplex	Low sensitivity than interferometers
		PS-FBG[85,86]	Enhanced sensitivity of FBG	Expensive than normal FBG
Transformer temperature (<150°C)	R-OTDR[92,93]		Distributed sensing	Low spatial resolution (meter-level)
	FBG[94–101]		High spatial resolution (centimeter level)	Quasidistributed sensing, limited test points
Hydrogen in the transformer oil (detection range: 50 to 2000 ppm, temperature range 30 to 110°C)[131]	FBGs (H_2 absorption-induced stress on FBG)	With Pd films[119,123]	Sensitivity can be optimized by the thickness and the material of the film	Pd or Pd-based composite films are required to absorb H_2
		With Pd/Ag film[120,121]		
		With Pd/Au film[122]		
		With Pd/Cr film[123]		
		With Pd/Ti film[124,125]		
	Modified FBGs	D-shape FBGs with Pd films[126–128]	Enhanced sensitivity than normal FBGs	Polish or etched process is required
		etched FBGs with Pd films[129]		
	Reflectivity-based scheme (fiber endface)	WO$_3$-Pd film on fiber endface[130] PTFE-Pd film on fiber endface[131]	Small size and low cost	Multilayer films on the fiber end face are required
	PCF-based interferometer with Pd films[132] (H_2 absorption-induced stress)		Temperature-insensitive	SMF-PCF-SMF structure is required

sensing is a superior choice because of its intrinsic advantages as well as the extensive applications of OPGW and OPPC as shown in Fig. 14. There are optical fiber cables inside, which can be used as the distributed sensing fiber directly by utilizing the characteristic optical scattering effects.

2.4.1 Temperature monitoring

The temperature along the transmission lines is a crucial parameter because it affects the ampacity of overhead transmission lines. The common temperature measurement of
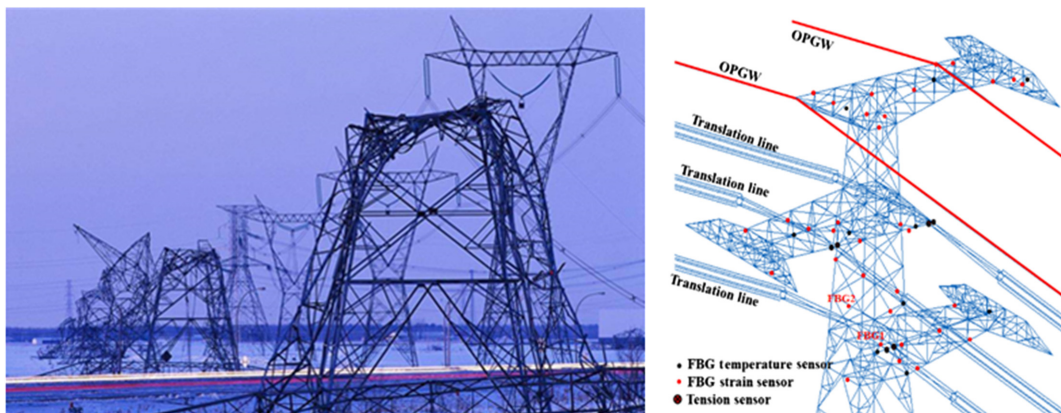

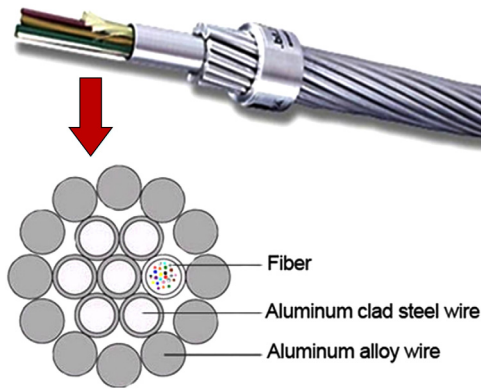**Fig. 13** Schematic diagram of power tower and FBG-based sensing system.

Fig. 14 Schematic diagram of OPPC/OPGW.

Fig. 15 Icing of transmission lines.

transmission lines includes noncontact infrared technology[143] and direct measurement through the surface electronic thermometer.[144,145] However, these methods easily interact with strong electromagnetic interference from the transmission line and require additional power. Nowadays, optical fiber sensors become an effective method to measure the temperature distribution of the transmission lines. Generally speaking, two kinds of optical fiber temperature sensing schemes, the point sensing and distributed fiber-optic sensing, have been applied in transmission lines.

B-OTDR[146] based on the Brillouin frequency shift with temperature of optical fiber has been used to realize the online temperature monitoring of three-phase cables with OPPC/OPGW. The experimental results showed that the temperature difference between the three-phase cables and the optical fiber inside is 0.018°C. R-OTDR[147] system with the temperature accuracy of ±1°C was used to measure the temperature of 400/50 OPPC with different actual working conditions of current-carrying capacity, wind velocity, and environment temperature. B-OTDR-based distributed temperature sensor for localizing the lightning stroke-induced temperature change in OPGW was also reported.[148]

FBGs[149,150] with portable systems were also used in temperature monitoring of transmission lines and they demonstrated a higher accuracy of ~0.1°C and greater stability. An FBG-based temperature measurement system was installed on No. 44 tower of 110-kV Zhengzhou transmission line in Luzhou, China.[151] The FBG system was a quasidistributed sensing technology and needed to inscribe the FBG in the optical fiber, which is not fully matched with OPPC/OPGW and limit its application.

2.4.2 Icing monitoring

Heavy ice coating of overhead transmission lines, as shown in Fig. 15, imposes a serious threat to the safe operation of power grids, such as conductor breakage, insulator flashover, and tower collapse. Numerous theoretical icing models have been developed to create reliable tools for predicting the features of icing process.[152]

Many methods including climatological data method, image method, load cell method, have been developed to monitor the ice load of overhead transmission lines. For the conventional electrical load cell used in ice monitoring, it is easily disturbed by strong electromagnetic interference, and it usually needs a power supply. The optical fiber load

cell has been widely applied in monitoring the ice coating of overhead transmission lines without these problems.

Ogawa et al.[153] presented an FBG load cell for ice monitoring on overhead transmission lines and carried out the tension experiment to acquire the relationship between the load and strain. To solve the cross sensitivity of strain and temperature, an unforced FBG is usually used as a comparison sensor. An FBG-based sensing system realized online icing monitoring on the 44# tower of 110-kV Zhenzou power grid.[154] An overhead conductor tension sensor based on FBG[155,156] was connected to the tower and the insulator with metallic clamps to monitor the icing-induced tension of 110-kV high-tension transmission line in Zhaotong, Yunnan province. The experiment results indicated that the tension sensitivity of the FBG sensor was 9.8 pm/kN and shows a good repeatability. A distributed online temperature and strain fiber sensing system based on the combination of B-OTDR and FBG were also proposed[157] and shown in Fig. 16. The B-OTDR sensing system is used to measure the temperature of overhead lines and the FBG sensing system is adopted to measure the tension of overhead lines.

To improve the performance of FBG-based icing monitoring system, some structures were designed for load cell.[158–164] Elastic element with two near-elliptical-shaped concavities structure[161] and coupled dual-beam ("S" beam) structure,[162] which is shown in Figs. 17(a) and 17(b), respectively, can be worked in harsh environments with a good sensitivity and resolution. The shearing structure with additional grooves as elastic element of load cell was designed to detect the eccentric load and temperature simultaneously.[163,164] Two vertically FBGs were mounted onto the additional grooves to eliminate temperature effects on strain measurement without extra FBG.

Some analysis models were also proposed by researchers.[165–167] A correction factor of gravity acceleration was added and greatly improved measurement performance in windy weather.[165] A strain difference model achieved absolute stress change values by measure the line sag difference constant of two points.[166,167] Experiment in Xuefeng mountain of Hunan shows that the strain difference model is superior to the traditional calculation method and can be applied on monitoring ice thickness of transmission lines.

Wydra et al.[168] presented a method that monitors the state of a transmission lines based on chirped FBG (CFBG) sensors. Compared to the uniform FBG, the linearly CFBG has a more considerable variation in wavelength, which would be
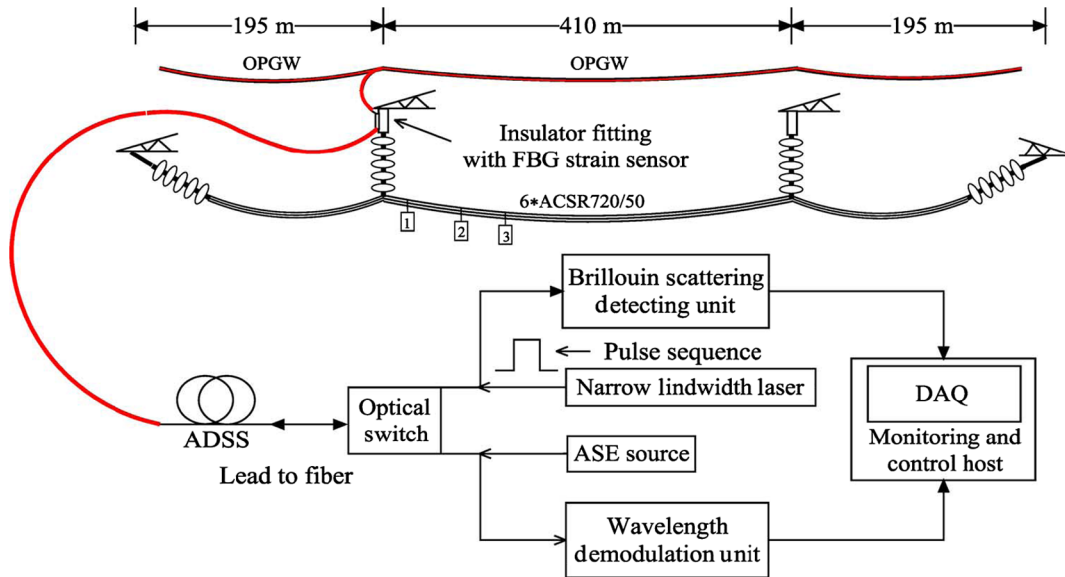
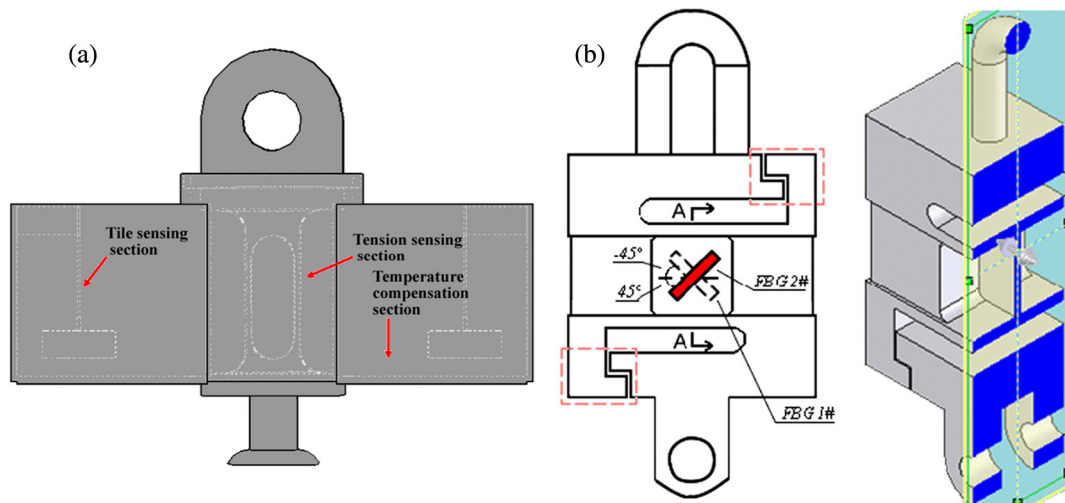**Fig.16** Schematic diagram of galloping monitoring based on FBG sensors.[157]

Fig.17 (a) Elastic element with two near-elliptical-shaped concavities structure[161] and (b) elastic element with coupled dual-beam ("S" beam) structure.[162]

used to improve the sensitivity and accuracy. In the presented CFBG sensor, temperature can be compensated by the spectrum shift.

2.4.3 Galloping monitoring

Transmission line galloping is wind-induced vibration of both single and bundle overhead conductors with low frequency (typically 0.1 to 3 Hz) and large amplitude (about 5 to 300 times of the power transmission lines diameter), which usually occurs in a specific environment with strong winds and transmission lines icing and lasts for several hours. Galloping may reduce air gaps between conductors, occasionally causing flashovers and repeated power supply interruptions, which is really harmful for power grid.[169]

Galloping has been studied for many years in theory and experiment, and many measures have been developed.[170,171] However, the galloping of transmission lines under different circumstances has not been accurately studied. The experimental method is an effective way to study the mathematical model of galloping or to verify the device to prevent flashovers.[172] Therefore, there is a great need for an effective online galloping monitoring system. The commonly used galloping monitoring techniques are camera and electrical accelerometers. However, these methods are susceptible to high-voltage environment and require power supply for monitoring devices. Optical fiber sensing technology maybe overcomes these limitations and plays a more and more important role in real-time monitoring. Moreover, OPPC/OPGW applied widely in transmission lines accelerates the process.

Bjerkan[173] monitored the vibrations of a 160-m span of a 60-kV line by FBG sensors gluing on the phase conductor. Huang et al.[174] investigated an FBG strain sensor on the phase conductor to measure its tension. Rui et al. designed a two-dimensional FBG-based acceleration sensor to
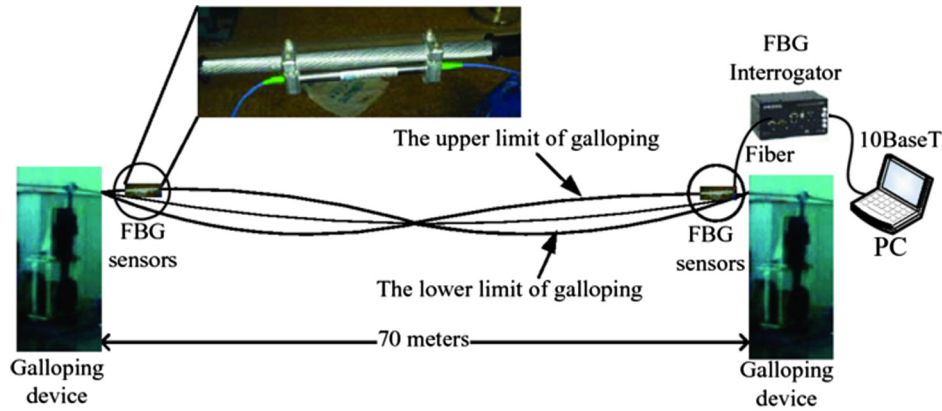
Fig.18 Schematic diagram of galloping monitoring based on FBG sensors.[176]

monitor the power transmission line galloping.[175] Chen et al.[176] used FBG-based strain sensor and temperature sensor to monitor the galloping of an overhead power transmission line. FBG sensors were installed on both ends of the OPGW cable, which can be seen from Fig. 18. The experiment results showed that the galloping amplitude could be obtained accurately in real time.

Hao et al.[157] developed a distributed online temperature and strain fiber sensing system based on the combined B-OTDR and FBG technology. The temperature of the transmission lines was monitored by B-OTDR, whereas the tension of the transmission lines was measured by FBG sensing system. The experimental line simulated the actual transmission line of Yun-Guang ± 80 kV DC transmission project. The experiments showed that Brillouin scattering and the FBG reflected signal would not affect each other. The transmission line load variation could be measured effectively and accurately by the FBG tension sensor.

A dynamic tension detection system composed of FBG tension sensors, OPGW, and a wavelength interrogator, as shown in Fig. 19, was designed to detect the galloping of overhead transmission lines.[177] The FBG tension sensor was installed between an insulator string and power tower

to monitor the dynamic tension of the phase conductor. A series of experiments at the State Grid Key Laboratory of Power Overhead Transmission Line Galloping proved its feasibility.

In summary, transmission lines are one of the most important parts in a power grid system but easily affected by weathering, such as icing and wind blowing. In addition, the excessive temperature rise will cause high-power energy loss and some accidents during high-voltage transmission process. Table 3 illustrated the optical fiber sensing technology applied on power towers and transmission lines. Two main fiber-optic sensing technologies applied in transmission lines are the FBG sensing and distributed sensing technologies. FBG sensors are more stable and cheaper and portable demodulation system. In contrast, the distributed sensing technology requires a highly demanding light source and a demodulator, but it can utilize the fiber in OPPC/OPGW directly without extra packaging and installation processes. Any point information along the OPPC/OPGW can be measured by distributed sensing technologies. The sensing cost is reduced dramatically and could be a trend for the health monitoring of long-distance transmission lines.
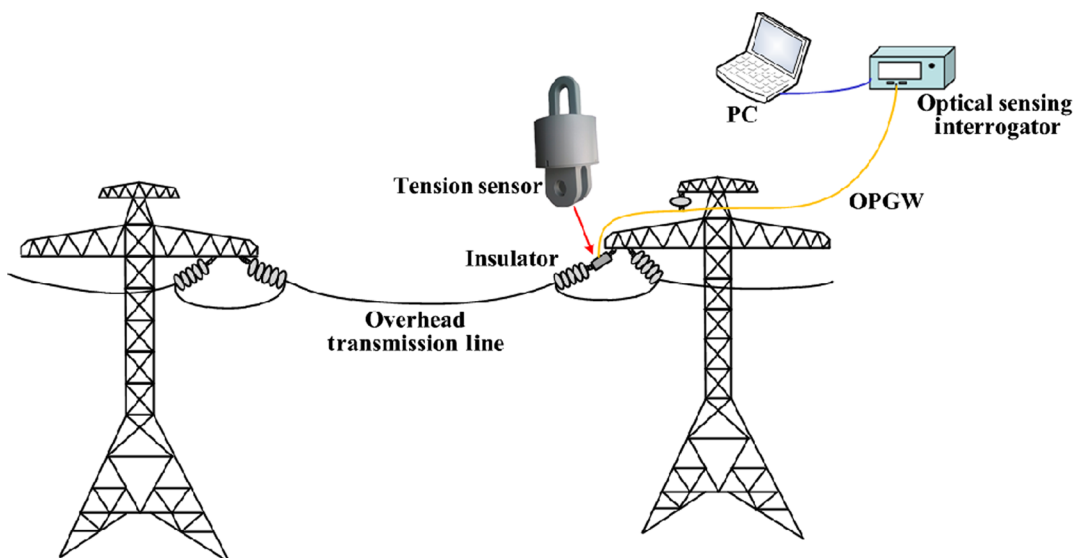

Fig.19 Schematic diagram of galloping monitoring system.[177]

Table 3 Optical fiber sensing technology applied on power towers and transmission lines.

Monitoring targets	Fiber-optic sensing technology		Characteristics
Stress, tilt, and deformation of power towers		FBGs[133–142] (with different packaging and installation schemes)	A standard measurement but temperature compensation is needed
Temperature in the transmission lines		R-OTDR/B-OTDR[146–148] (combined with OPPC/OPGW)	Distributed sensing with meter-level spatial resolution
		FBGs[149–151]	Quasidistributed sensing with centimeter-level spatial resolution
Icing on transmission lines (stress and temperature change)	FBGs	FBGs[153–156,158–167] (tension-induced strain measurement)	Stable but temperature compensation needed
		FBGs combined with B-OTDR[157] (tension-induced strain measurement)	Matched with OPPC and OPGW
		Chirp FBGs[168] (strain with temperature compensation)	Strain and temperature simultaneously difficult to multiplexing
Conductor motion (galloping mainly)	FBGs	Strain-based[173–177]	High stability but limited by sensor numbers
		Acceleration-based[175]	

2.5 Other Applications

Equivalent salt deposit density (ESDD) can reflect the contamination condition of the insulator. Monitoring ESDD is useful to evaluate the contamination condition and clean of the insulator. An FBG sensor for detecting ESDD on insulators of power transmission lines was reported.[178] By additional polyimide layers, FBG is sensitive to humidity and salt. An optical intensity attenuation-based ESDD monitoring system was carried out in real transmission lines.[179] The experiment results indicated that the error of the sensors was <10%.

An FBG sensing system for wind speed measurement of transmission lines was reported in Ref. 180. To overcome the cross sensitivity, two FBGs were glued on the two surfaces of the beam used to measure wind induced the force. The experiment results that the measurement error of the wind speed was less than ±0.5 m/s.

Oliveira et al.[181–183] developed a fiber-optic sensor system to monitor the current leakage of glass-type insulator strings in Brazil power towers. Six leakage current sensors were installed: two on a 230-kV tower and four on two 500-kV towers. Combined the information of current leakage and the environmental humidity, they could infer the degree of pollution on insulator strings. Leakage current reached high-peak levels during washing the insulator strings. They also inferred the effectiveness of the washing from the leakage current after drying of the insulator strings.

2.6 Comparison of the Sensing Technologies Applied in Power Grid

We reviewed fiber-optic sensing applications in the main components of a power grid, including transformers, power tower, and overhead transmission lines. Additionally, there are many other sensing technologies applied in power grid. Table 4 summarized the advantages and disadvantages of typical sensing technology applied in power grids. Compared to the other sensing technologies applied in power gird, fiber-optic sensing technology shows some advantages, including immunity of electromagnetic interference, capabilities of multiplexing and distributed sensing, and tolerance to harsh environments, which has great potential in power grids.

3 Perspective of Fiber-Optic Sensing-Based Intelligent Early Fault Diagnosis System

Nowadays, the applications of fiber-optic sensing technology in power grids are still at the stage of experimental verification and training. As mentioned above, lots of works have been done in monitoring transformers, power towers, or transmission lines, respectively. Few papers demonstrated the consideration of a whole fiber-optic sensing network to realize an intelligent early fault diagnosis system for a power grid, which appears to be the development trend. Our group has been carrying on a long-term project to realize such an early fault diagnosis subsystem.[184,185] The subsystem consists of the analysis and the sensing parts based on distributed and quasidistributed fiber-optic sensors such as FBG, R-OTDR, and Φ-OTDR. Up to now, part of the subsystem for power towers and transmission lines has been built up and worked for two years in a power grid located in Jianshan, Henan province.

The intelligent early fault diagnosis system, including Φ-OTDR-based transmission line galloping measurement, R-OTDR-based DTS for transmission lines and transformers, FBG-based strain and tilt sensing for towers, and FBG-based bolt loosening sensing for towers and transformer structures, is shown in Fig. 20. The optical fiber integrated in OPPC/OPGW transmission lines between #3 tower and #9 tower combined with Φ-OTDR and R-OTDR technologies were used to monitor the temperature and galloping of the 4-km transmission lines. The health monitoring of #6 tensile tower was based on 94 FBG strain sensors in order to accumulate its detail behaviors for different loads, which is not necessary for a minimum system. More than 10 FBG-based intelligent bolts have been built up and will be installed on the #6 towers and transformer soon to observe the bolt loosening process. The R-OTDR-based temperature

Table 4 Sensing technologies applied in power grid.

|	Methods	Advantages	Disadvantages
Temperature	Thermometer	Low cost, traditional method	Low accuracy, strong electromagnetic interference
	Infrared	Simple measurement process	Strong electromagnetic interference, additional power supply
	Fiber-optic sensors	High-sensitivity, immune electromagnetic interference, distributed sensing	Additional light source, high cost of demodulation system for BOTDR or φOTDR
Structure health	Strain gauges	Low cost	Hard to multiplex, electromagnetic interference
	Fiber-optic sensors	Compact size, easy to multiplex	Require a suitable package
Gas	Chromatography	Commercial instrument	Offline measurement
	Spectroscopy	Commercial instrument	Offline measurement
	Electrochemical sensors	Online monitoring, low cost	Strong electromagnetic interference, risks of shorts and sparks
	Fiber-optic sensors	Online monitoring, low cost	
Icing	Image method		Effected by the heavy snow
	Climatological data method	Developed for years to predict the ice loading	Not accurate
	Electrical load cell	Easily calculated using the measured tension	Strong electromagnetic interference, additional power supply
	Fiber-optic sensors	Easy to multiplex, immune electromagnetic interference	Require a suitable package
Galloping	Camera	Remote sensing by a GPRS network	Difficult to cover a complete span, short lifetime of camera in harsh environment
	Acceleration or tension sensor	Directly measurement	Strong electromagnetic interference, additional power supply
	Fiber-optic sensors	Immune electromagnetic interference, use OPGW/OPPC naturally	Additional light source, high cost of demodulation system
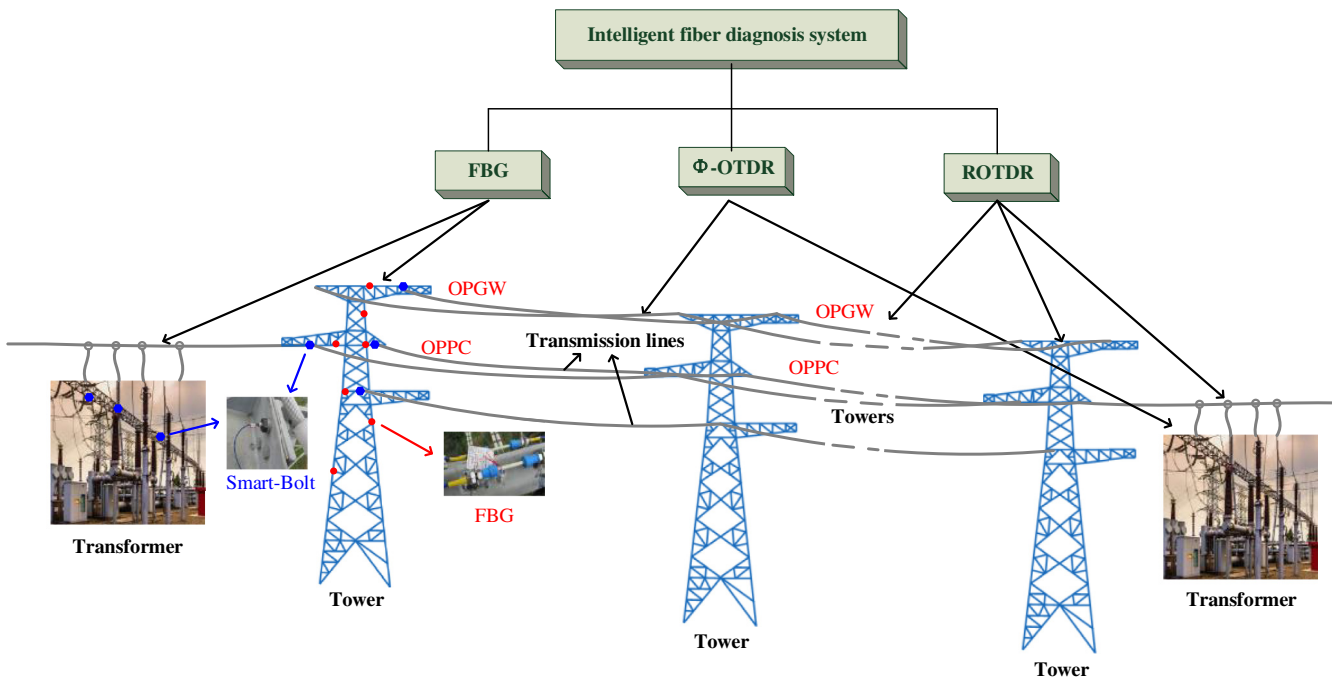
Fig. 20 Intelligent fiber early fault diagnosis system in power grid monitoring.
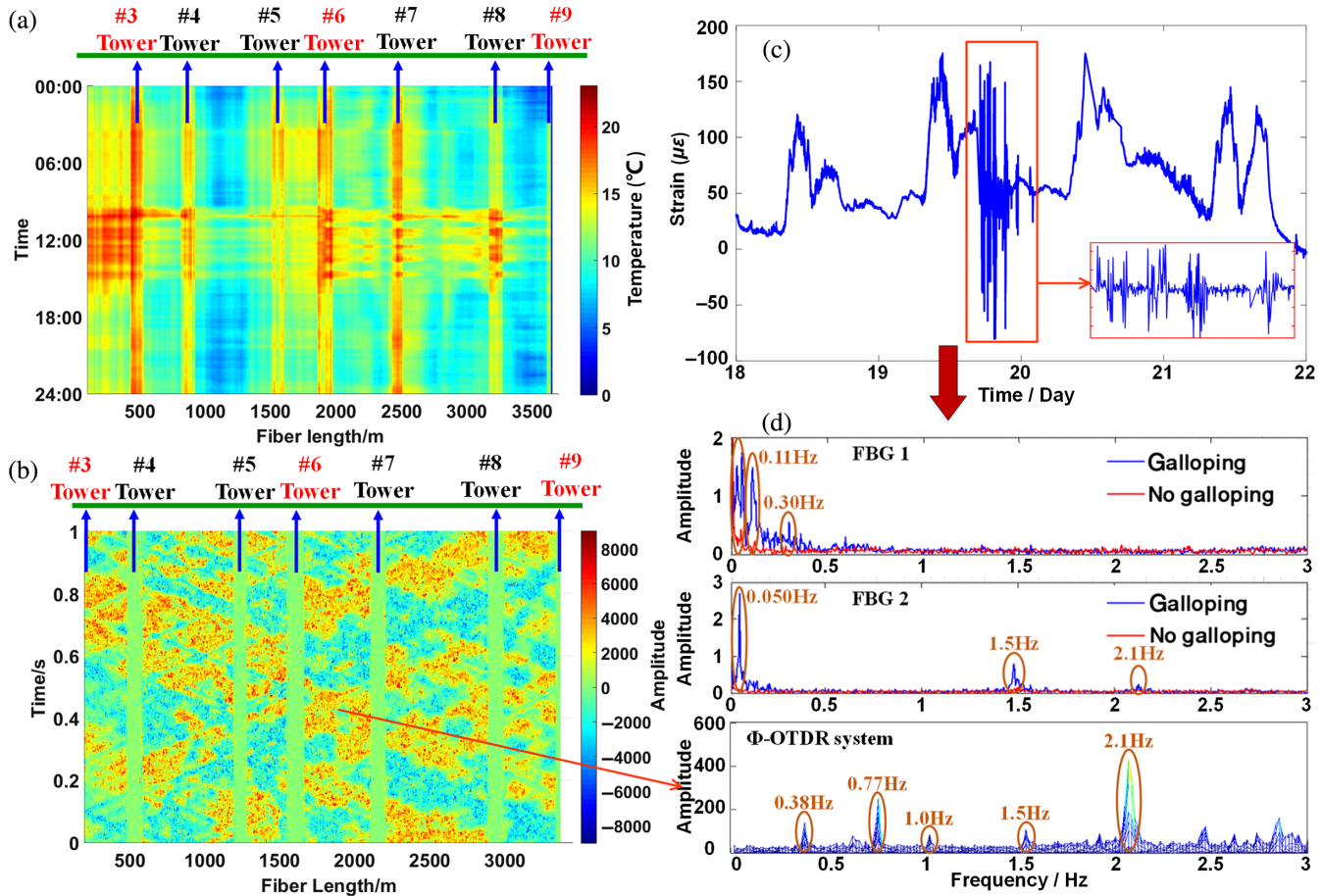
Fig. 21 (a) Time-domain signals from R-OTDR system, (b) time-domain signals from Φ-OTDR system; (c) time-domain signals from FBG strain sensor, and (d) frequency-domain signals from FBG strain sensor and Φ-OTDR system.

sensors and the FBG-based strain and hydrogen sensors were planned to be installed in the transformer. The whole fiber optical sensing system would be finished and worked as a network in two years and the diagnosis program would be realized based on enough experimental data.

Some typical experimental results are shown in Fig. 21. Figure 21(a) illustrated the temperature of the 4-km long transmission line monitored by R-OTDR. The temperature is higher at noon, which can be understand easily. There is obvious temperature difference between the suspended transmission line and the transmission line fixed on a tower. Sun and wind are the two main reasons. The tower is constructed by the angle steels with the gray color, which absorbs more heat and leads to higher temperature. On the other hand, wind cools the suspended transmission lines more than with the coiled cables fixed on towers. It can be readily understood that the temperature of suspended transmission line is lower than that of the lines fixed on towers. In addition, the temperature of tower 5 is lower than the other towers. The main reason we believed is that the tower 5 is located at the top of the mountain and the wind is stronger. The galloping of the transmission lines was monitored by Φ-OTDR and one example is shown in Fig. 21(b) demonstrating the obvious galloping frequency. In Fig. 21(d), the FBG-based strain sensor installed on #6 tower also observed the transmission line galloping-induced dynamic strain on the tower, as labeled in Fig. 21(c). FBG1 are

installed at C phase hanging line of #6 tensile tower, and FBG2 are installed at #6 tensile tower body (shown in Fig. 13). FBG strain sensors at different positions showed the difference in frequency, but the FBGs closed to the galloping transmission line gave the same frequencies, such as 1.5 and 2.1 Hz, as those of Φ-OTDR. The lower frequency of 0.05 Hz is the harmonic frequency of the #6 tower.

Combining different optic-sensing technologies and applying them collaboratively in power grids, more comprehensive, and reliable information can be obtained for monitoring the power grids. This is the development trend of the future and an excellent opportunity of fiber-optic sensing technology in smart power grids.

4 Conclusions

We reviewed the fiber-optic sensing in the health monitoring of power grids in the past 20 years. The relevant fiber-optic sensing technologies, including FBGs, fiber-optic interferometers, OTDR, Φ-OTDR, B-OTDR, B-OTDA, and R-OTDR, were reflected in terms of their operational principles, respectively. Their applications were classified by the components of the power grid (e.g., transformers, power tower, and overhead transmission lines). For transformers, fiber-optic sensors were used to monitor the early fault symptoms of partially charge, hydrogen, and thermal abnormities. For power towers, their strain, tilt, and deformation

were detected by FBG-based sensors. The galloping induced by icing and wind blowing, the stress concentration, and temperature abnormity of transmission lines were measured by FBG and types of distributed fiber-optic sensors. A fiber-optic sensing-based early fault diagnosis system of power grids that was planned and built up partly in Henan were described, and some preliminary results emphasized a win–win collaboration of FBG and Φ-OTDR in terms of confirming the galloping event and evaluating the tower safety. Fiber-optic sensing-based early fault monitoring systems in power grids are being accelerated by the extensive applications of OPPC and OPGW. The costs of fiber-optic sensing in power grids are being reduced significantly and certainly awaiting for a huge market.

References

1. S. M. Kaplan, "Electric power transmission: background and policy issues," Report no R40511, US Congressional Research Service, Washington, D.C. (2009).
2. M. Majumder et al., "Fibre Bragg gratings in structural health monitoring—Present status and applications," *Sens. Actuators A: Phys.* **147**(1), 150–164 (2008).
3. J. Brownjohn, "Structural health monitoring of civil infrastructure," *Philos. Trans. R. Soc. London, Ser. A* **365**(1851), 589–622 (2007).
4. X. W. Ye, Y. H. Su, and J. P. Han, "Structural health monitoring of civil infrastructure using optical fiber sensing technology: a comprehensive review," *Sci. World J.* **2014**, 652329 (2014).
5. H. H. Zhu, B. Shi, and C. C. Zhang, "FBG-based monitoring of geohazards: current status and trends," *Sensors* **17**(3), 452 (2017).
6. C. Y. Hong et al., "Recent progress of using Brillouin distributed fiber-optic sensors for geotechnical health monitoring," *Sens. Actuators A: Phys.* **258**, 131–145 (2017).
7. K. Miah and D. K. Potter, "A review of hybrid fiber-optic distributed simultaneous vibration and temperature sensing technology and its geophysical applications," *Sensors* **17**(11), 2511 (2017).
8. H. Ohno et al., "Industrial applications of the BOTDR optical fiber strain sensor," *Opt. Fiber Technol.* **7**(1), 45–64 (2001).
9. Y. Qian et al., "Review of salinity measurement technology based on optical fiber sensor," *Sens. Actuators B: Chem.* **260**, 86–105 (2017).
10. I. García et al., "Optical fiber sensors for aircraft structural health monitoring," *Sensors* **15**(7), 15494–15519 (2015).
11. R. Di Sante, "Fibre optic sensors for structural health monitoring of aircraft composite structures: Recent advances and applications," *Sensors* **15**(8), 18666–18713 (2015).
12. S. J. Mihailov. "Fiber Bragg grating sensors for harsh environments," *Sensors* **12**(2), 1898–1918 (2012).
13. H. E. Joe et al., "A review on optical fiber sensors for environmental monitoring," *Int. J. Precis. Eng. Manuf. Green Technol.* **5**(1), 173–191 (2018).
14. P. Vaiano et al., "Lab on fiber technology for biological sensing applications," *Laser Photonics Rev.* **10**(6), 922–961 (2016).
15. F. Chiavaioli et al., "Biosensing with optical fiber gratings," *Nanophotonics* **6**(4), 663–679 (2017).
16. G. F. Moore, *Electric Cables Handbook: BICC Cables*, Blackwell Science, Oxford (2000).
17. X. Zhang et al., "Online monitoring of power transmission lines in smart grid based on distributed optical fiber sensing technology," *Optoelectron. Technol.* **37**(4), 221–229 (2017).
18. R. M. Silva et al., "Optical current sensors for high power systems: a review," *Appl. Sci.* **2**(3), 602–628 (2012).
19. C. Sun, P. R. Ohodnicki, and E. M. Stewart, "Chemical sensing strategies for real-time monitoring of transformer oil: a review," *IEEE Sens. J.* **17**(18), 5786–5806 (2017).
20. M. Amin and J. Stringer, "The electric power grid: today and tomorrow," *MRS Bull.* **33**(4), 399–407 (2008).
21. M. Wang, A. J. Vandermaar, and K. D. Srivastava, "Review of condition assessment of power transformers in service," *IEEE Electr. Insul. Mag.* **18**(6), 12–25 (2002).
22. E. Fernandez et al., "Review of dynamic line rating systems for wind power integration," *Renew. Sustainable Energy Rev.* **53**, 80–92 (2016).
23. R. Kashyap, *Fiber Bragg Gratings*, Academic Press, San Diego, California (1999).
24. A. Othonos and K. Kalli, *Fiber Bragg Gratings: Fundamentals and Applications in Telecommunications and Sensing*, Artech House, Boston, London (1999).
25. D. A. Krohn, T. MacDougall, and A. Mendez, *Fiber Optic Sensors: Fundamentals and Applications*, SPIE Press, Bellingham, Washington (2014).
26. B. H. Lee et al., "Interferometric fiber-optic sensors," *Sensors* **12**(3), 2467–2486 (2012).
27. T. Allsop et al., "A high sensitivity refractometer based upon a long period grating Mach–Zehnder interferometer," *Rev. Sci. Instrum.* **73**(4), 1702–1705 (2002).
28. L. V. Nguyen et al., "High temperature fiber sensor with high sensitivity based on core diameter mismatch," *Opt. Express* **16**(15), 11369–11375 (2008).
29. H. Y. Choi, M. J. Kim, and B. H. Lee, "All-fiber Mach–Zehnder type interferometers formed in photonic crystal fiber," *Opt. Express* **15**(9), 5711–5720 (2007).
30. P. Lu et al., "Tapered fiber Mach–Zehnder interferometer for simultaneous measurement of refractive index and temperature," *Appl. Phys. Lett.* **94**(13), 131110 (2009).
31. F. Pang et al., "In-fiber Mach–Zehnder interferometer based on double cladding fibers for refractive index sensor," *IEEE Sens. J.* **11**(10), 2395–2400 (2011).
32. D. W. Kim et al., "In-fiber reflection mode interferometer based on a long-period grating for external refractive-index measurement," *Appl. Opt.* **44**(26), 5368–5373 (2005).
33. Z. Tian, S. S. Yam, and H.-P. Loock, "Single-mode fiber refractive index sensor based on core-offset attenuators," *IEEE Photonics Technol. Lett.* **20**(16), 1387–1389 (2008).
34. K. S. Park et al., "Temperature robust refractive index sensor based on a photonic crystal fiber interferometer," *IEEE Sens. J.* **10**(6), 1147–1148 (2010).
35. L. Yuan, J. Yang, and Z. Liu, "A compact fiber-optic flow velocity sensor based on a twin-core fiber Michelson interferometer," *IEEE Sens. J.* **8**(7), 1114–1117 (2008).
36. J. Sirkis et al., "In-line fiber etalon for strain measurement," *Opt. Lett.* **18**(22), 1973–1975 (1993).
37. D. Hunger et al., "A fiber Fabry–Perot cavity with high finesse," *New J. Phys.* **12**(6), 065038 (2010).
38. Y.J. Rao et al., "Micro Fabry–Perot interferometers in silica fibers machined by femtosecond laser," *Opt. Express* **15**(21), 14123–14128 (2007).
39. X. Wan and H. F. Taylor, "Intrinsic fiber Fabry–Perot temperature sensor with fiber Bragg grating mirrors," *Opt. Lett.* **27**(16), 1388–1390 (2002).
40. V. Machavaram, R. Badcock, and G. Fernando, "Fabrication of intrinsic fibre Fabry–Perot sensors in silica fibres using hydrofluoric acid etching," *Sens. Actuators A: Phys.* **138**(1), 248–260 (2007).
41. J.R. Zhao et al., "High-resolution and temperature-insensitive fiber-optic refractive index sensor based on Fresnel reflection modulated by Fabry–Perot interference," *J. Lightwave Technol.* **28**(19), 2799–2803 (2010).
42. B. Culshaw, "The optical fibre Sagnac interferometer: an overview of its principles and applications," *Meas. Sci. Technol.* **17**(1), R1 (2005).
43. V. Passaro et al., "Gyroscope technology and applications: a review in the industrial perspective," *Sensors* **17**(10), 2284 (2017).
44. P. Gysel and R. K. Staubli, "Statistical properties of Rayleigh backscattering in single-mode fibers," *J. Lightwave Technol.* **8**(4), 561–567 (1990).
45. A. T. Young, "Rayleigh scattering," *Appl. Opt.* **20**(4), 533–535 (1981).
46. M. Born and E. Wolf, *Principles of optics: Electromagnetic Theory of Propagation, Interference and Diffraction of Light*, Elsevier, Amsterdam, Netherlands (2013).
47. I. L. Fabelinskii, *Molecular Scattering of Light*, Springer Science & Business Media, Boston, Massachusetts (2012).
48. M. Tateda et al., "First measurement of strain distribution along field-installed optical fibers using Brillouin spectroscopy," *J. Lightwave Technol.* **8**(9), 1269–1272 (1990).
49. A. Hartog, A. Leach, and M. Gold, "Distributed temperature sensing in solid-core fibres," *Electron. Lett.* **21**(23), 1061–1062 (1985).
50. J. Dakin et al., "Distributed optical fibre Raman temperature sensor using a semiconductor light source and detector," *Electron. Lett.* **21**(13), 569–570 (1985).
51. M. Barnoski and S. Jensen, "Fiber waveguides: a novel technique for investigating attenuation characteristics," *Appl. Opt.* **15**(9), 2112–2115 (1976).

52. S. Yin and T. Francis, *Fiber Optic Sensors*, Marcel Dekker Inc., New York (2002).
53. A. Barrias, J. R. Casas, and S. Villalba, "A review of distributed optical fiber sensors for civil engineering applications," *Sensors* **16**(5), 748 (2016).
54. H. F. Taylor and C. E. Lee, "Apparatus and method for fiber-optic intrusion sensing," Google Patents (1993).
55. Y. Lu et al., "Distributed vibration sensor based on coherent detection of phase-OTDR," *J. Lightwave Technol.* **28**(22), 3243–3249 (2010).
56. Z. Qin et al., "High sensitivity distributed vibration sensor based on polarization-maintaining configurations of phase-OTDR," *IEEE Photonics Technol. Lett.* **23**(15), 1091–1093 (2011).
57. F. Peng et al., "Ultra-long high-sensitivity Φ-OTDR for high spatial resolution intrusion detection of pipelines," *Opt. Express* **22**(11), 13804–13810 (2014).
58. Y. Wang et al., "Real-time distributed vibration monitoring system using Φ-OTDR," *IEEE Sens. J.* **17**(5), 1333–1341 (2017).
59. T. Kurashima, H. Tsuneo, and T. Mitsuhiro, "Distributed-temperature sensing using stimulated Brillouin scattering in optical silica fibers," *Opt. Lett.* **15**(18), 1038–1040 (1990).
60. X. Bao et al., "Experimental and theoretical studies on a distributed temperature sensor based on Brillouin scattering," *J. Lightwave Technol.* **13**(7), 1340–1348 (1995).
61. M. Nikles, L. Thévenaz, and P. A. Robert, "Simple distributed temperature sensor based on Brillouin gain spectrum analysis," *Proc. SPIE* **2360**, 138–141 (1994).
62. T. R. Parker et al., "A fully distributed simultaneous strain and temperature sensor using spontaneous Brillouin backscatter," *IEEE Photonics Technol. Lett.* **9**(7), 979–981 (1997).
63. K. Shimizu et al., "Coherent self-heterodyne Brillouin OTDR for measurement of Brillouin frequency shift distribution in optical fibers," *J. Lightwave Technol.* **12**(5), 730–736 (1994).
64. S. Uchida, E. Levenberg, and A. Klar, "On-specimen strain measurement with fiber-optic distributed sensing," *Measurement* **60**, 104–113 (2015).
65. C. A. Galindez-Jamioy and J. M. Lopez-Higuera, "Brillouin distributed fiber sensors: an overview and applications," *J. Sens.* **2012**, 1–17 (2012).
66. C. K. Leung et al., "Optical fiber sensors for civil engineering applications," *Mater. Struct.* **48**(4), 871–906 (2015).
67. M. C. Farries and A. J. Rogers, "Distributed sensing using stimulated Raman interaction in a monomode optical fiber," *Proc. SPIE* **0514**, 121–132 (1984).
68. L. Schenato, "A review of distributed fibre optic sensors for geo-hydrological applications," *Appl. Sci.* **7**(9), 896 (2017).
69. International Electrotechnical Commission (IEC) standard, "High-voltage test techniques: partial discharge measurements," https://webstore.iec.ch/preview/info_iec60270%7Bed3.0%7Db.pdf, IEC-60270 (2000).
70. J. P. Fracarolli et al., "Fiber-optic interferometric method for acoustic emissions detection on power transformer's bushing," in *SBMO/IEEE MTT-S Int. Microwave & Optoelectron. Conf. (IMOC)*, pp. 1–5 (2013).
71. C. Macià-Sanahuja, J. García-Souto, and H. Lamela-Rivera, "Characterization of an ultrasonic low frequency fibre optic interferometric sensor for partial discharges detection in transformers," in *Proc. Int. Topical Meeting Opt. Sens. and Artif. Vision*, pp. 157–163 (2004).
72. J. Posada-Roman, J. A. Garcia-Souto, and J. Rubio-Serrano, "Fiber-optic sensor for acoustic detection of partial discharges in oil-paper insulated electrical systems," *Sensors* **12**(4), 4793–4802 (2012).
73. J. Posada, J. Garcia-Souto, and J. Rubio-Serrano, "Multichannel optical-fibre heterodyne interferometer for ultrasound detection of partial discharges in power transformers," *Meas. Sci. Technol.* **24**(9), 094015 (2013).
74. T. Zhang et al., "A fiber-optic sensor for acoustic emission detection in a high voltage cable system," *Sensors* **16**(12), 2026 (2016).
75. Q. Yu and X. Zhou, "Pressure sensor based on the fiber-optic extrinsic Fabry–Perot interferometer," *Photonic Sens.* **1**(1), 72–83 (2011).
76. J. Deng et al., "Optical fiber sensor-based detection of partial discharges in power transformers," *Opt. Laser Technol.* **33**(5), 305–311 (2001).
77. B. Yu et al., "Fiber Fabry–Perot sensors for detection of partial discharges in power transformers," *Appl. Opt.* **42**(16), 3241–3250 (2003).
78. S. E. Lima et al., "Fiber Fabry–Perot sensors for acoustic detection of partial discharges in transformers," in *IEEE 8th Int. Conf. Prop. Appl. Dielectr. Mater.*, pp. 307–311 (2009).
79. S. E. Lima et al., "Intrinsic and extrinsic fiber Fabry–Perot sensors for acoustic detection in liquids," *Microw. Opt. Technol. Lett.* **52**(5), 1129–1134 (2010).
80. J. Lee and S. Lee, "Applied sound frequency monitoring in the transformer oil using fiber-optic Sagnac interferometer," *J. Acoust. Soc. Korea* **34**(4), 288–294 (2015).
81. L. Wang et al., "A fiber-optic PD sensor using a balanced Sagnac interferometer and an EDFA-Based DOP Tunable fiber ring laser," *Sensors* **14**(5), 8398–8422 (2014).
82. B. Sarkar et al., "Condition monitoring of high voltage transformers using Fiber Bragg Grating Sensor," *Measurement* **74**, 255–267 (2015).
83. B. Sarkar et al., "Intensity-modulated fiber Bragg grating sensor for detection of partial discharges inside high-voltage apparatus," *IEEE Sens. J.* **16**(22), 7950–7957 (2016).
84. S. E. Lima et al., "Mandrel-based fiber-optic sensors for acoustic detection of partial discharges—A proof of concept," *IEEE Trans. Power Delivery* **25**(4), 2526–2534 (2010).
85. S. E. Lima et al., "Fiber laser sensor based on a phase-shifted chirped grating for acoustic sensing of partial discharges," *Photonic Sens.* **3**(1), 44–51 (2013).
86. G.M. Ma et al., "Distributed partial discharge detection in a power transformer based on phase-shifted FBG," *IEEE Sens. J.* **18**(7), 2788–2795 (2018).
87. International Electrotechnical Commission (IEC) Standard, "IEC 60076-7 power transformers part 7: loading guide for oil-immersed power transformers," https://webstore.iec.ch/preview/info_iec60076-7%7Bed1.0%7Den_d.pdf, December (2005).
88. A. Lefevre et al., "3-D computation of transformers overheating under nonlinear loads," *IEEE Trans. Magn.* **41**(5), 1564–1567 (2005).
89. M. Pradhan and T. Ramu, "Prediction of hottest spot temperature (HST) in power and station transformers," *IEEE Trans. Power Delivery* **18**(4), 1275–1283 (2003).
90. M. Pradhan and T. Ramu, "Estimation of the hottest spot temperature (HST) in power transformers considering thermal inhomogeniety of the windings," *IEEE Trans. Power Delivery* **19**(4), 1704–1712 (2004).
91. S. Tenbohlen et al., "Diagnostic measurements for power transformers," *Energies* **9**(5), 347 (2016).
92. G. Nokes, "Optimising power transmission and distribution networks using optical fibre distributed temperature sensing systems," *Power Eng. J.* **13**(6), 291–296 (1999).
93. A. Ukil, H. Braendle, and P. Krippner, "Distributed temperature sensing: review of technology and applications," *IEEE Sens. J.* **12**(5), 885–892 (2012).
94. D. Jia, Z. Yao, and C. Li, "The transformer winding temperature monitoring system based on fiber Bragg grating," *Int. J. Smart Sens. Intell. Syst.* **8**(1), 538–560 (2015).
95. D. Kweon and K. Koo, "Winding temperature measurement in a 154 kV transformer filled with natural ester fluid," *J. Electr. Eng. Technol.* **8**(1), 156–162 (2013).
96. E. Pinet, S. Ellyson, and F. Borne, "Temperature fiber-optic point sensors: commercial technologies and industrial applications," in *Proc. 46th Int. Conf. Microelectron. Devices Mater. (MIDEM 2010)*, pp. 31–43 (2010).
97. D. Kweon et al., "A study on the hot spot temperature in 154kv power transformers," *J. Electr. Eng. Technol.* **7**(3), 312–319 (2012).
98. D. Kweon et al., "Hot spot temperature for 154 kV transformer filled with mineral oil and natural ester fluid," *IEEE Trans. Dielectr. Electr. Insul.* **19**(3), 1013–1020 (2012).
99. R. Gong et al., "Analysis and experiment of hot-spot temperature rise of 110 kV three-phase three-limb transformer," *Energies* **10**(8), 1079 (2017).
100. J. G. Deng et al., "Hot-spot temperature and temperature decay rate measurement in the oil immersed power transformer through FBG based quasi-distributed sensing system," *Microwave Opt. Technol. Lett.* **59**(2), 472–475 (2017).
101. A. Y. Arabul, F. K. Arabul, and I. Senol, "Experimental thermal investigation of an ONAN distribution transformer by fiber-optic sensors," *Electr. Power Syst. Res.* **155**, 320–330 (2018).
102. IEEE Standard, "IEEE guide for the interpretation of gases generated in oil-immersed transformers," in *IEEE Standard C57.104-2008*, pp. 1–36 (2009).
103. G. Belanger and M. Duval, "Monitor for hydrogen dissolved in transformer oil," *IEEE Trans. Electr. Insul.* **EI-12**(5), 334–340 (1977).
104. Y. Leblanc et al., "Determination of dissolved gases and furan-related compounds in transformer insulating oils in a single chromatographic run by headspace/capillary gas chromatography," *J. Chromatogr. A* **657**(1), 111–118 (1993).
105. C. Zhang and F. Wang, "Application of photo-acoustic spectroscopy technology to dissolved gas analysis in oil of oil-immersed power transformer," *Gaodianya Jishu/High Voltage Eng.* **31**(2), 84–86 (2005).
106. W.-G. Chen et al., "Analysis of infrared absorption properties of dissolved gases in transformer oil," *Zhongguo Dianji Gongcheng Xuebao/Proc. Chin. Soc. Electr. Eng.* **28**(16), 148–153 (2008).
107. T. Waitz et al., "Ordered mesoporous In_2O_3: synthesis by structure replication and application as a methane gas sensor," *Adv. Funct. Mater.* **19**(4), 653–661 (2009).
108. J. Zhang et al., "Hierarchically porous ZnO architectures for gas sensor application," *Cryst. Growth Des.* **9**(8), 3532–3537 (2009).
109. W. Zeng et al., "Hydrogen sensing and mechanism of M-doped SnO_2 (M = Cr^{3+}, Cu^{2+}, and Pd^{2+}) nanocomposite," *Sens. Actuator B-Chem.* **160**(1), 455–462 (2011).
110. W. Chen et al., "Pd-doped SnO_2-based sensor detecting characteristic fault hydrocarbon gases in transformer oil," *J. Nanomater.* **2013**, 1–9 (2013).

111. S. K. Mishra et al., "Surface plasmon resonance-based fiber-optic methane gas sensor utilizing graphene-carbon nanotubes-poly(methyl methacrylate) hybrid nanocomposite," *Plasmonics* **10**(5), 1147–1157 (2015).

112. M. Benounis et al., "Study of a new evanescent wave optical fibre sensor for methane detection based on cryptophane molecules," *Sens. Actuator B-Chem.* **107**(1), 32–39 (2005).

113. S. Wu et al., "Mode-filtered light methane gas sensor based on cryptophane A," *Anal. Chim. Acta* **633**(2), 238–243 (2009).

114. C. Tao et al., "Optical fiber sensing element based on luminescence quenching of silica nanowires modified with cryptophane-A for the detection of methane," *Sens. Actuator B-Chem.* **156**(2), 553–558 (2011).

115. G. Yan et al., "Fiber-optic acetylene gas sensor based on microstructured optical fiber Bragg gratings," *IEEE Photonics Technol. Lett.* **23**(21), 1588–1590 (2011).

116. X. Wang et al., "C$_2$H$_2$ gas sensor based on Ni-doped ZnO electrospun nanofibers," *Ceram. Int.* **39**(3), 2883–2887 (2013).

117. A. Bychkov, S. Korobeynikov, and A. Y. Ryzhkina, "Determination of the hydrogen diffusion coefficient in transformer oil," *Tech. Phys.* **56**(3), 421–422 (2011).

118. F. Yang, D. Jung, and R. M. Penner, "Trace detection of dissolved hydrogen gas in oil using a palladium nanowire array," *Anal. Chem.* **83**(24), 9472–9477 (2011).

119. M. Fisser et al., "Development of hydrogen sensors based on fiber Bragg grating with a palladium foil for online dissolved gas analysis in transformers," *Proc. SPIE* **10329**, 103292P (2017).

120. M. Butler, R. Sanchez, and G. Dulleck, *Fiber Optic Hydrogen Sensor*, Sandia National Laboratories, Albuquerque (1996).

121. G. Ma et al., "Pd/Ag coated fiber Bragg grating sensor for hydrogen monitoring in power transformers," *Rev. Sci. Instrum.* **86**(4), 045003 (2015).

122. P. Ohodnicki, J. Baltrus, and T. Brown, "Pd/SiO2 and AuPd/SiO2 nanocomposite-based optical fiber sensors for H2 sensing applications," *Sens. Actuators B: Chem.* **214**, 159–168 (2015).

123. M. R. Samsudin et al., "Fiber Bragg gratings hydrogen sensor for monitoring the degradation of transformer oil," *IEEE Sens. J.* **16**(9), 2993–2999 (2016).

124. G. Ma et al., "High sensitive and reliable fiber Bragg grating hydrogen sensor for fault detection of power transformer," *Sens. Actuators B: Chem.* **169**, 195–198 (2012).

125. G. Ma et al., "Fiber Bragg grating sensor for hydrogen detection in power transformers," *IEEE Trans. Dielectr. Electr. Insul.* **21**(1), 380–385 (2014).

126. Y. T. Luo et al., "Research on high sensitive D-shaped FBG hydrogen sensors in power transformer oil," *Sensors* **16**(10), 1641 (2016).

127. J. Dai et al., "Side-polished fiber Bragg grating hydrogen sensor with WO$_3$-Pd composite film as sensing materials," *Opt. Express* **19**(7), 6141–6148 (2011).

128. J. Jiang et al., "Highly sensitive dissolved hydrogen sensor based on side-polished fiber Bragg grating," *IEEE Photonics Technol. Lett.* **27**(13), 1453–1456 (2015).

129. J. Jiang et al., "Note: dissolved hydrogen detection in power transformer oil based on chemically etched fiber Bragg grating," *Rev. Sci. Instrum.* **86**(10), 106103 (2015).

130. J. Dai et al., "Improved performance of fiber-optic hydrogen sensor based on WO3-Pd2Pt-Pt composite film and self-referenced demodulation method," *Sens. Actuators B: Chem.* **249**, 210–216 (2017).

131. T. Mak et al., "Optical fiber sensor for the continuous monitoring of hydrogen in oil," *Sens. Actuators B: Chem.* **190**, 982–989 (2014).

132. Y. Zhang et al., "Photonic crystal fiber modal interferometer with Pd/WO3 coating for real-time monitoring of dissolved hydrogen concentration in transformer oil," *Rev. Sci. Instrum.* **87**(12), 125002 (2016).

133. Z. L. Xue et al., "FBG Strain sensor for monitoring daily wind direction change on power tower cross arm deformation effects," *Adv. Mater. Res.* **645**, 334–337 (2013).

134. D. L. Li et al., "Application of fiber Bragg grating earth pressure sensor in safety monitoring for electric steel tower foundation," *Adv. Mater. Res.* **709**, 365–369 (2013).

135. J. F. Geng et al., "Research on a fiber Bragg grating strain sensor for tower vibration," *Appl. Mech. Mater.* **496-500**, 1373–1375 (2014).

136. J. Geng et al., "The comparison and analysis of fiber grating strain sensor and resistance strain slice for transmission tower vibration monitoring," *Appl. Mech. Mater.* **533**, 211–213 (2014).

137. Q. Xie and C. Yan, "Wind tunnel test on 1000 kV UHV AC double circuit transmission tower-conductor coupling system," *Gaodianya Jishu/High Voltage Eng.* **36**(4), 900–906 (2010).

138. Q. Xie, C. Yan, and S. Li, "Wind tunnel lest analysis on dynamic tension of 1000 kV UHV eight bundled conductors," *Gaodianya Jishu/High Voltage Eng.* **36**(7), 1594–1600 (2010).

139. Q. Xie, C. Yan, and Y. Zhang, "Experiment and analysis on wind-induced dynamic tension of ice covered UHV conductors," *Gaodianya Jishu/High Voltage Eng.* **36**(8), 1865–1870 (2010).

140. Y. X. Cao et al., "Design and application of online landslide monitoring system for transmission lines corridor based on the optical fiber sensing technology," *Appl. Mech. Mater.* **556-562**, 3160–3163 (2014).

141. C. Deng et al., "A case study of landslide monitoring system for a transmission tower in Maoxian, Sichuan China," in *IEEE 9th Int. Conf. Commun. Software and Networks (ICCSN)*, pp. 1516–1519 (2017).

142. X. Huang et al., "An online monitoring technology of tower foundation deformation of transmission lines," *Struct. Health Monit.* (2018).

143. X. Zhu et al., "An autonomous obstacles negotiating inspection robot for extra-high voltage power transmission lines," in *9th Int. Conf. Control, Autom. Rob. and Vision*, pp. 1–6 (2006).

144. B. Sheng and W. Zhou, "Ultra-low power wireless-online-monitoring platform for transmission line in smart grid," in *Int. Conf. High Voltage Eng. and Appl. (ICHVE)*, pp. 244–247 (2010).

145. Z. Yao et al., "Transmission line temperature online monitoring system based on ZigBee," in *Int. Conf. Sustainable Power Gener. and Supply, SUPERGEN'09*, pp. 1–4 (2009).

146. Y. Hao et al., "Online temperature monitoring in power transmission lines based on Brillouin optical time domain reflectometry," *Optik-Int. J. Light Electron Opt.* **126**(19), 2180–2183 (2015).

147. J. Tong et al., "Research on Raman-OTDR sensing-based optical phase conductor (OPPC) temperature monitoring and the section temperature field," *Proc. SPIE* **9044**, 904405 (2013).

148. L. Lu et al., "Experimental study on location of lightning stroke on OPGW by means of a distributed optical fiber temperature sensor," *Opt. Laser Technol.* **65**, 79–82 (2015).

149. Y. Cheng, X. Tian, and C. Li, "Using fiber Bragg grating sensor on ice monitoring on electric power transmission lines. Part I: the measurement of the temperature," in *Int. Conf. High Voltage Eng. and Appl. (ICHVE)*, pp. 256–259 (2010).

150. J. Shi, "The research of power cable online measurement system based on fiber Bragg grating sensor," *Chem. Eng. Trans.* **51**, 1255–1260 (2016).

151. S. Liu et al., "Temperature measurements for transmission lines ASED on passive optical sensing," *Appl. Mech. Mater.* **543-547**, 1035–1041 (2014).

152. K. Savadjiev and M. Farzaneh, "Modeling of icing and ice shedding on overhead power lines based on statistical analysis of meteorological data," *IEEE Trans. Power Delivery* **19**(2), 715–721 (2004).

153. Y. Ogawa, J.-I. Iwasaki, and K. Nakamura, "A multiplexing loadmonitoring system of power transmission lines using fiber Bragg grating," in *Conf. Opt. Fiber Sens.*, p. OThC16 (1997).

154. F. L. Liu et al., "Application of fiber Bragg grating device in icing monitoring system of transmission lines," *Appl. Mech. Mater.* **543–547**, 1030–1034 (2014).

155. S. B. Liang et al., "An overhead conductor weighing sensor based on fiber Bragg grating," *Appl. Mech. Mater.* **462–463**, 32–38 (2014).

156. H. L. Yang et al., "Research and application of optical fiber sensing technology on high voltage transmission line monitoring," *Appl. Mech. Mater.* **462–463**, 59–63 (2014).

157. J. Luo et al., "Development of optical fiber sensors based on Brillouin scattering and FBG for online monitoring in overhead transmission lines," *J. Lightwave Technol.* **31**(10), 1559–1565 (2013).

158. G. Ma et al., "A fiber Bragg grating tension and tilt sensor applied to icing monitoring on overhead transmission lines," *IEEE Trans. Power Delivery* **26**(4), 2163–2170 (2011).

159. G. Ma et al., "Design of fiber Bragg grating load sensor used in ice monitoring on overhead transmission lines," in *Int. Conf. High Voltage Eng. and Appl. (ICHVE)*, pp. 232–235 (2010).

160. G. Ma et al., "Ice monitoring system of transmission lines based on fiber Bragg grating sensor," in *Int. Conf. High Voltage Eng. and Appl. (ICHVE)*, pp. 684–687 (2010).

161. G. Ma et al., "Ice monitoring on overhead transmission lines with FBG tension sensor," in *Power and Energy Eng. Conf. (APPEEC)*, pp. 1–4 (2010).

162. G. Ma et al., "A novel optical load cell used in icing monitoring on overhead transmission lines," *Cold Reg. Sci. Technol.* **71**, 67–72 (2012).

163. N. Mao et al., "High sensitive FBG load cell for icing of overhead transmission lines," in *Opt. Fiber Sens. Conf. (OFS)*, pp. 1–4 (2017).

164. G. Ma et al., "The reusable load cell with protection applied for online monitoring of overhead transmission lines based on fiber Bragg grating," *Sensors* **16**(6), 922 (2016).

165. M. Zhang et al., "Design and experiment of FBG-based icing monitoring on overhead transmission lines with an improvement trial for windy weather," *Sensors* **14**(12), 23954–23969 (2014).

166. Z. Liu, "Application of strain difference model and FBG sensor to power transmission line ice monitoring," in *Asia Commun. and Photonics Conf.*, p. ASu2A. 138 (2015).

167. Z. M. Liu, Z. G. Zhang, and L. M. Li, "Research on monitoring ice thickness of overhead lines based on FBG sensor and parabolic method," *Adv. Mater. Res.* **1044-1045**, 854–857 (2014).

168. M. Wydra et al., "Overhead transmission line sag estimation using a simple optomechanical system with chirped fiber Bragg gratings. Part 1: preliminary measurements," *Sensors* **18**(1), 309 (2018).

169. M. Farzaneh, "Ice accretions on high-voltage conductors and insulators and related phenomena," *Philos. Trans. R. Soc. London, Ser. A* **358**(1776), 2971–3005 (2000).

170. J. Wang and J.-L. Lilien, "Overhead electrical transmission line galloping. A full multi-span 3-DOF model, some applications and design recommendations," *IEEE Trans. Power Delivery* **13**(3), 909–916 (1998).

171. M. Lu et al., "Hybrid nutation damper for controlling galloping power lines," *IEEE Trans. Power Delivery* **22**(1), 450–456 (2007).

172. P. Van Dyke and A. Laneville, "Galloping of a single conductor covered with a D-section on a high-voltage overhead test line," *J. Wind Eng. Ind. Aerodyn.* **96**(6-7), 1141–1151 (2008).

173. L. Bjerkan, "Application of fiber-optic Bragg grating sensors in monitoring environmental loads of overhead power transmission lines," *Appl. Opt.* **39**(4), 554–560 (2000).

174. Q. Huang et al., "New type of fiber-optic sensor network for smart grid interface of transmission system," in *Power and Energy Soc. Gen. Meeting*, IEEE, pp. 1–5 (2010).

175. X. Rui et al., "Online monitoring system on power transmission line galloping based on fiber grating sensors," in *30th Chin. Control Conf. (CCC)*, pp. 4327–4330 (2011).

176. Y. Chen, Z. Zhang, and X. Chen, "Novel monitoring method of power transmission line galloping based on fiber Bragg grating sensor," *Opt. Eng.* **50**(11), 114403 (2011).

177. G. Ma et al., "A fiber Bragg grating-based dynamic tension detection system for overhead transmission line galloping," *Sensors* **18**(2), 365 (2018).

178. G. Ma et al., "High sensitive FBG sensor for equivalent salt deposit density measurement," *IEEE Photonics Technol. Lett.* **27**(2), 177–180 (2015).

179. X.-B. Huang, C. Xie, and H. Li, "Equivalent salt deposit density optical fiber sensor for transmission lines in power grid," *IEEE Sens. J.* **17**(1), 91–99 (2017).

180. G. Ma et al., "A passive optical fiber anemometer for wind speed measurement on high-voltage overhead transmission lines," *IEEE Trans. Instrum. Meas.* **61**(2), 539–544 (2012).

181. E. Fontana et al., "Novel sensor system for leakage current detection on insulator strings of overhead transmission lines," *IEEE Trans. Power Delivery* **21**(4), 2064–2070 (2006).

182. S. C. Oliveira, E. Fontana, and F. J. D. M. de Melo, "Leakage current activity on glass-type insulators of overhead transmission lines in the northeast region of Brazil," *IEEE Trans. Power Delivery* **24**(2), 822–827 (2009).

183. S. C. Oliveira, E. Fontana, and F. J. D. M. de Melo, "Real-time monitoring of the leakage current of 230-kV glass-type insulators during washing," *IEEE Trans. Power Delivery* **24**(4), 2257–2260 (2009).

184. K. Xie et al., "Transmission line galloping induced dynamic strain measurement of an angle brace based power transmission tower by FBG sensors," in *IEEE Int. Instrum. Meas. Technol. Conf. (I2MTC)*, pp. 1–5 (2018).

185. K. Xie et al., "Structural health monitoring of power transmission system based on optical fiber sensor under transmission line galloping," *Laser Optoelectron. Prog.* **55**(7), 070606 (2018).

Quan Chai received his BS degree in optical information science and technology in 2008, his MS degree in optical engineering in 2011, and his PhD in mechatronic engineering in 2016, all from Harbin Engineering University. He is currently a lecturer in the Key Laboratory of In-Fiber Integrated Optics of Ministry of Education of Harbin Engineering University. His current research interests include special fibers, optical fiber sensors, and their applications.

Yang Luo received his BS degree in physics from the Northeast Forestry University, Heilongjiang, China, in 2016. He is currently pursuing his MS degree in optics at Harbin Engineering University, Heilongjiang, China. His current research interests include optical sensors, measurement, and systems.

Jing Ren received his PhD in materials science and technology in 2009 from Pardubice University, Czech. He is currently a professor in the Key Laboratory of In-Fiber Integrated Optics of Ministry of Education of Harbin Engineering University. His current research interests include laser glasses and optical fiber amplifiers.

Jianzhong Zhang received his BS degree in condensed matter physics from Lanzhou University, his MS degree and his PhD in optical engineering from Harbin Engineering University. He has been a professor at the College of Science of Harbin Engineering University since 2012 and published more than 90 papers in refereed journals and conferences, edited 2 books, and held more than 10 patents. His research interests include optical fiber devices, optical fiber sensing technologies, and their applications.

Jun Yang received his BS degree in optoelectronics, his MEng degree in optical engineering, and his PhD in photonics from Harbin Engineering University, Harbin, China, in 1999, 2002, and 2005, respectively. He is currently a professor in the Key Laboratory of In-Fiber Integrated Optics of the Ministry Education of China at Harbin Engineering University. His current research interests include fiber-optic sensors and optic interferometers.

Libo Yuan received his BS degree in physics from Heilongjiang University, his MEng degree in communication and electronic systems from Harbin Engineering University, and his PhD in photonics from Hong Kong Polytechnic University. He has authored or co-authored more than 240 refereed international journal papers and holds more than 120 patents related to fiber-optic technology. His current research interests include fiber-based laser trapping systems, in-fiber integrated optics, fiber-optic sensors, and their applications.

Gang-Ding Peng received his BSc degree in physics from Fudan University in 1982 and his MSc degree in applied physics and PhD in electronic engineering from Shanghai Jiao Tong University in 1984 and 1987, respectively. He has been working at University of New South Wales, Australia, since 1991. He is a fellow and life member of both OSA and SPIE. His research interests include optical fibers and devices, fiber sensors, and nonlinear optics.